



Norwegian University of  
Science and Technology

# Recycling of Fine Silicon Particles for Solar Grade Silicon Production

**Matthew Engel Wermers**

Materials Science and Engineering (MSMT)

Submission date: June 2018

Supervisor: Jafar Safarian, IMA

Norwegian University of Science and Technology  
Department of Materials Science and Engineering



## Acknowledgements

This project could not have been completed without the support and help of mentors, coaches, and friends. I would first like to thank my supervisor Jafar Safarian, he has helped me this last year with many aspects of this project. I would also like to thank Adrian Murgau, the industry contact that has provided valuable real-world insight. This work was performed within the Research Centre for Sustainable Solar Cell Technology, co-sponsored by the Norwegian Research Council and research and industry partners. Another sincere thank you to the SiManTi group in the Department of Materials Science and Engineering. This student group provided great understanding and valuable feedback all while keeping me accountable for my work. My last thanks goes out to my friends and family for providing constant support even though they are on the other side of the globe.

## Abstract

The production of solar grade silicon wafers results in 50% wasted silicon. Due to the high volume of waste, recycling the fines into a useable material allows for use of all this valuable silicon. Currently there is no reuse/recycle technology used in the solar silicon process. The purpose of the research is to create a reuse/recycle technology. The experimental procedures used consisted of: characterizing the silicon fines used, producing two kinds of silicon agglomerates, green agglomeration strength was tested, and indurated agglomeration strength was tested. Four characterizing tests were completed on the silicon fines; X-Ray Diffraction (XRD), Scanning Electron Microscopy (SEM), particle size analysis, and Inductively coupled plasma mass spectrometry (ICP-MS). The results of this testing indicated the fines were crystalline silicon. In order to make the two kinds silicon agglomerates in the lab, compressed briquettes were made along with pellets. Briquettes were formed by uniaxial pressing. A variety of briquettes were made using different amounts of water. The size of briquettes that were pressed were 10mm×10mm. Once the briquettes were produced, a drop test was performed to determine the strength. This property is important because the pellet must be able to survive all of its post producing handling without breaking. From the results of the initial testing it can be seen that the optimal water content is in the upper range of 8-10%. Next, briquettes were pressed with three different binders in three different amounts. These briquettes with a binder were tested from their green strength by using the same drop test. Here we see that increased binder amount does not equal increased green strength. After the green briquettes were tested, they were next indurated in the oven, and their strength was looked at. The indurated briquettes that were looked at are briquettes pressed with water and briquettes pressed with a binder. The drop test was used to check the strength. It can be seen that increased drying time, will increase the strength of the briquette. Lastly, a small batch of pellets was created with a pelletizing drum. Two sizes of pellets were created with a binder, and their strength was measured using the drop test. It shows that these pellets, both green and indurated have a lesser strength compared to the briquettes that were created.

## Table of Contents

### Acknowledgements

### Abstract

<b>1</b>	<b>Introduction</b>	<b>7</b>
<b>2</b>	<b>Theory and Background</b>	<b>9</b>
2.1	Overview of the solar silicon production	9
2.2	Value chain of silicon production	15
2.3	Cutting and wafering of solar silicon	16
2.4	Solar silicon waste	18
2.5	Agglomeration theory and practice	18
2.6	Pelletizing principles	20
<b>3</b>	<b>Experimental procedure</b>	<b>23</b>
3.1	Characterization of silicon fine powder	23
3.2	Characterization of microsilica	23
3.3	Making agglomerates by press	24
3.4	Making briquettes with binders by press	25
3.5	Strength test for green briquettes	26
3.6	Induration of green briquettes	26
3.7	Strength test for indurated briquettes	27
3.8	Making agglomerates by pelletizing	27
3.9	Induration of green pellets	28
3.10	Strength test for pellets	28

<b>4</b>	<b>Results and Discussion</b>	<b>29</b>
4.1	Characteristics of silicon particles	29
4.2	Characteristics of microsilica particles	31
4.3	Strength of green briquettes	33
4.4	Strength of green briquettes with binder	36
4.5	Strength of indurated briquettes	39
4.6	Strength of green pellets	47
4.7	Strength of indurated pellets	49
<b>5</b>	<b>Conclusions and future work</b>	<b>51</b>
<b>6</b>	<b>References</b>	<b>53</b>

## List of Figures

Figure 2.1:Submerged Arc Furnace .....	9
Figure 2.2: Simplified furnace model .....	10
Figure 2.3: Siemens Process .....	12
Figure 2.4: Production amounts for different solar silicon .....	13
Figure 2.5: Schematic overview of the Czochralski process .....	14
Figure 2.6: Monocrystalline ingot on the left and multicrystalline ingot on the right.....	15
Figure 2.7: Value chain for solar silicon.....	15
Figure 2.8: Proposed value chain.....	16
Figure 2.9: Lifetime map .....	16
Figure 2.10: Multiwire saw.....	17
Figure 2.11: Sintering productivity in relation to grain size.....	20
Figure 2.12: Increase in a production of pellets over time .....	21
Figure 2.13: Capillary forces on green balls.....	22
Figure 3.1: Material provided by REC Solar, silicon fines on left, microsilica on right.....	23
Figure 3.2: Uniaxial press schematic .....	24
Figure 3.3: Mixing the combination of water and silicon fines with the use of steel balls .....	24
Figure 3.4: Hand press that was used to produce the briquettes.....	25
Figure 3.5: Pelletizing Disk .....	27
Figure 4.1: XRD mapping of silicon.....	29
Figure 4.2: Particle size distribution of the fine silicon .....	30
Figure 4.3: SEM of the fine silicon.....	30
Figure 4.4: XRD mapping of microsilica .....	32
Figure 4.5: Particle size distribution of the microsilica .....	32
Figure 4.6: SEM of microsilica.....	33
Figure 4.7: First break number of green briquettes.....	34
Figure 4.8: Press error, “lip” formed on the left, and broken “lip” on the right .....	35
Figure 4.9: Shatter number of green pellets.....	35
Figure 4.10: Shatter number with varied applied load.....	36
Figure 4.11: First break number of green briquettes with binder .....	38
Figure 4.12: Shatter number of green briquettes with binder .....	38
Figure 4.13: Comparison of briquettes, water vs organic binder, dried at 60°, first break .....	40
Figure 4.14: Comparison of briquettes, water vs organic binder, dried at 60°, shatter .....	41
Figure 4.15: First break of briquettes with 2 wt% binder, dried at 80° .....	43
Figure 4.16: Shatter of briquettes with 2 wt% binder, dried at 80° .....	43
Figure 4.17: First break of briquettes with 4 wt% binder, dried at 80° .....	44
Figure 4.18: Shatter of briquettes with 4 wt% binder, dried at 80° .....	44
Figure 4.19: First break of briquettes with 6 wt% binder, dried at 80° .....	45
Figure 4.20: Shatter of briquettes with 6 wt% binder, dried at 80° .....	45
Figure 4.21: Comparison of drying temperature, 2 wt% binder, first break.....	46
Figure 4.22: Comparison of drying temperature, 2 wt% binder, Shatter.....	46
Figure 4.23: Briquettes dried at 80° on the left, Briquettes dried at 60° on the right.....	47
Figure 4.24: Example of pellets that were produced .....	48
Figure 4.25: First break of dried pellets, 6 wt% binder, 80° .....	49
Figure 4.26: Shatter of dried pellets, 6 wt% binder, 80° .....	50

## List of Tables

Table 2.1: Comparison of sawing methods.....	18
Table 2.2: Comparison of size and shape for three agglomeration processes .....	20
Table 3.1: Summary of briquettes made with binder.....	26
Table 4.1: ICP-MS results for silicon .....	31
Table 4.2: Drop test results for green briquettes made with water .....	34
Table 4.3: Drop test results for green briquettes made with binder.....	37
Table 4.4: Mass loss of briquettes dried at 60° .....	39
Table 4.5: Mass loss of briquettes dried at 80° .....	42
Table 4.6: Drop test results for green pellets .....	48
Table 4.7: Mass loss of pellets dried at 80° .....	49

## 1 Introduction

The global demand of energy is on the rise. It is estimated that the total world energy consumption will rise by 28% by 2040 [1]. While renewable energy sources are expected to be the fastest growing, fossil fuels are expected to account for more than 75% of the energy use in 2040 [1]. While fossil fuels are created over time from the decomposition of dead plants and animals, it takes millions of years. The increased demand for energy is causing strains on the supply of fossil fuels and running out of them is concerning. In addition to the concerns about availability, there are significant health concerns about the emissions from fossil fuels use.

China is one of the largest consumers of fossil fuels and continues to battle poor air quality. Photographs from many in its largest cities consistently show the residents wearing respiration masks. According to reports from the World Health Organization (WHO), poor air quality was the cause of more than 1 million deaths in China in 2012, and low and middle-income countries also experience high death rates due to air quality. The WHO goes on to report that 92% of the world's population lives in places where the air quality exceeds WHO limits [2]. This is causing a healthcare crisis. The limited availability and healthcare crisis caused by fossil fuels are creating the right time for the increased development and use of renewable energy sources.

Renewable energy sources are broad and include many different sources. The most basic definition of renewable energy is, "Energy that is generated from natural processes that are continuously replenished" [3]. Solar power is a renewable energy source. Currently solar power or photovoltaics supplies 1.3% of the global power generation [4]. While 1.3% may not seem very big, that number has more than doubled in the last three years. From this growth, it is easy to see that solar power is on the rise and the production of solar cells is becoming an important industry for today and for many years to come.

The history of the solar cell goes back further than one may think. It goes all the way back to 1839 when the photovoltaic effect was first discovered. Later, the first solar cell was created in 1883, but was not produced commercially until 1956 [5]. The continued growth in solar energy brings a focus on the manufacturing of the silicon cells used in the renewable energy. Solar cell manufacturing is increasing year after year with no signs of slowing down. In 2016, the world saw a 32% growth in gigawatts produced from photovoltaics [6]. In 2017, it saw a 31% growth in production [7]. By 2018, there is a predicted growth rate of 27% [8]. With this constant increase in production it is important to know that large amounts of waste are also being produced. During the squaring, cutting, and wafering of the silicon there is on average 40 - 50% waste of the total ingot [9]. Currently there are not many things being done with all this waste of fine silicon particles. The ability to recycle the fine silicon particles into solar grade silicon reduces waste and

takes the value of this renewable energy to the next level. This thesis intends to investigate a method to create a reuse/recycle technology in the solar silicon process. By following the ideas that were used in the iron industry; agglomeration of silicon fines to be used in the production process was explored.

## 2 Theory and Background

### 2.1 Overview of the solar silicon production

A solar cell can be made from any semiconductor, and in today's market, silicon is the most used material for solar cells. Silicon is the second most abundant element in the earth's crust, making up approximately 28% and is usually found in the form of quartz ( $\text{SiO}_2$ ) or silicates [10]. This is because silicates are the most stable form due to the high affinity of Si and O atoms. In order to produce a silicon semiconductor, the silicon needs to be refined. Through many different processing steps which will be described below,  $\text{SiO}_2$  from quartz is transformed into pure silicon needed for the production of solar cells. The first step taken is to produce what is known as "Metallurgical grade" silicon (MG-Si). MG-Si is produced from  $\text{SiO}_2$  by carbothermic reduction in a submerged arc furnace. The resulting MG-Si is between 96-98% pure silicon. The idealized reaction that is taking place in the furnace is:



A typical submerged arc furnace used to produce MG-Si can be seen in the figure 2.1 below:

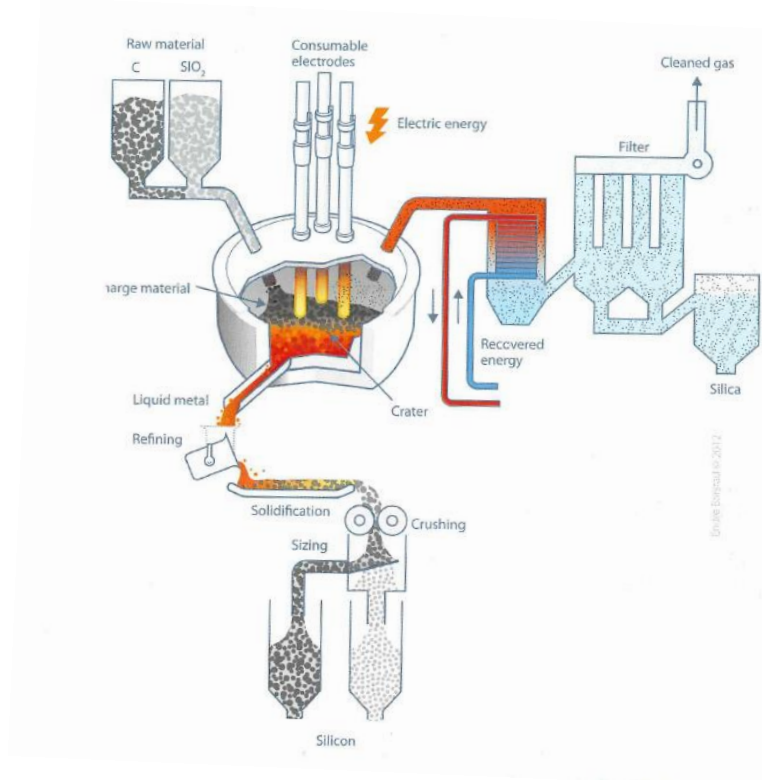


Figure 2.1: Submerged Arc Furnace

A submerged arc furnace (SAF) is used for this process, not a blast furnace (which is typically used for the production of iron) because a blast furnace cannot reach the high temperature needed for the reduction of silicon. There are a few different configurations for an SAF, but the most common for the silicon process is a three-phase alternating current, with the electrodes in an equilateral triangle formation [11]. When looking at figure 2.1, it can be seen that the SiO<sub>2</sub> is added with carbon at the top of the furnace and the MG-Si is tapped from the bottom. Figure 2.1 may look like a simple reaction, but the process is very complex. In order to understand what is going on in the furnace, the furnace can be viewed as divided into two different zones. A low temperature zone in the top half of the furnace and a high temperature zone in the lower half. In these two different zones, five reactions are taking place to produce the MG-Si. To get a better look at what is happening in the furnace, a simplified model is shown in figure 2.2.

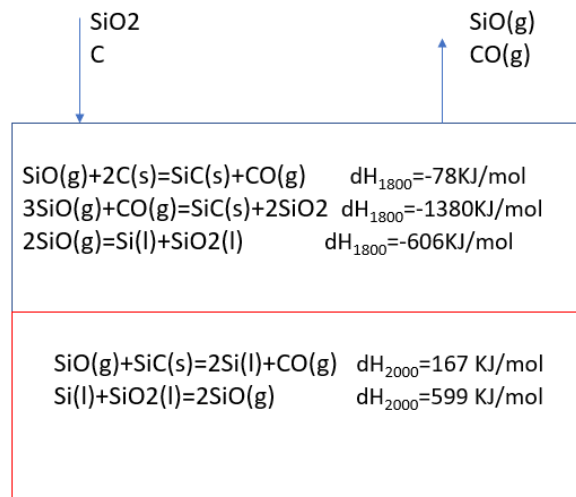


Figure 2.2: Simplified furnace model

In figure 2.2, the low temperature zone is on top with three reactions taking place. Looking at the thermodynamics of the three reactions, it can be seen that all three enthalpies are negative. The three reactions taking place in the low temperature zone are exothermic, this means that they are giving heat. By giving heat to the system they are helping pre-heat the charging of the raw materials in the furnace. Temperatures in the top zone can range between 700 to 1300 degrees Celsius [12]. The two reactions taking place in the high temperature zone, on the bottom, both have a positive enthalpy, meaning that the reactions are endothermic, absorbing heat. Temperatures in the lower zone reach approximately 2000 degrees Celsius [12]. When adding the raw materials at the top, it is important to not add too much carbon. Too much carbon, will cause the formation of SiC particles and these will build up in the furnace [12]. In order for the furnace to run at its best efficiency, SiC should not be produced in the lower part of the furnace. When looking at both figure 2.1 and figure 2.2 one sees that SiO gas leaves through the top of the furnace.

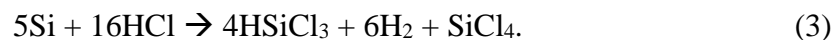
When this SiO gas undergoes oxidation, it will form SiO<sub>2</sub> particles known as microsilica as seen in the equation below.



The SiO<sub>2</sub> is formed through condensation and collects through the top. These microsilica particles have a uniform size and shape with an average size being ~15µm [12]. This is an important by-product used in many different industries. When the MG-Si is ready to leave the furnace, it is in liquid form and taken out from the bottom of the furnace. While this carbothermic process to produce MG-Si in principle is defined as a slag free process, slag is created and also tapped from the bottom of the furnace [11]. The MG-Si liquid and slag are tapped into a ladle and further refined with oxygen [12]. Because most of the impurity elements are more noble than the MG-Si being tapped, conventional refining processes are very difficult. When refining the ladle with oxygen, the amount of slag generated depends on the amount of impurities that have been introduced with the feed. When oxygen is added to the liquid, it will cause the impurities to oxidize and form a slag layer. This slag layer is immiscible with the liquid MG-Si and easy to remove. The slag refining is a great process for the removal of boron, calcium, and aluminium from the liquid melt [13]. Once the MG-Si has been removed from the slag, it can be cooled and solidified.

In order to produce the silicon needed for use in a semiconductor for solar cells, the silicon needs to be +99.9999% (6N) pure. The MG-Si from the previous section, is only 96-98% pure, and after ladle refining it is around 99% Si, thus it must be further purified. There are two main routes to go from MG-Si to solar grade silicon (SoG-Si); the chemical route and the metallurgical route. The chemical route is more commonly referred to as the Siemens process and is the commercially preferred method. The metallurgical route is the more common method in Norway and used by REC Solar [12], known so far as ELKEM Solar process. This report will look briefly at both methods.

The siemens process, as seen in figure 2.3 [12], can be simplified to three steps; gasification of MG-Si, distillation, and deposition of Si [5]. Using MG-Si as the raw material it is mixed with hydrochloric acid at elevated temperatures (~300° C). This will produce a gaseous mixture of Si, H, and Cl. The gas is then collected and cooled into a liquid. The equation for this reaction is:



The distillation step is used to remove impurities, the most important impurity being removed in this step is boron. Boron is very harmful to electrical properties of SoG-Si. After distillation, the product is silane gas and that will go on to the last step. During this last step, the silane gas is heated, and this will produce solid Si and hydrogen in the following reaction:

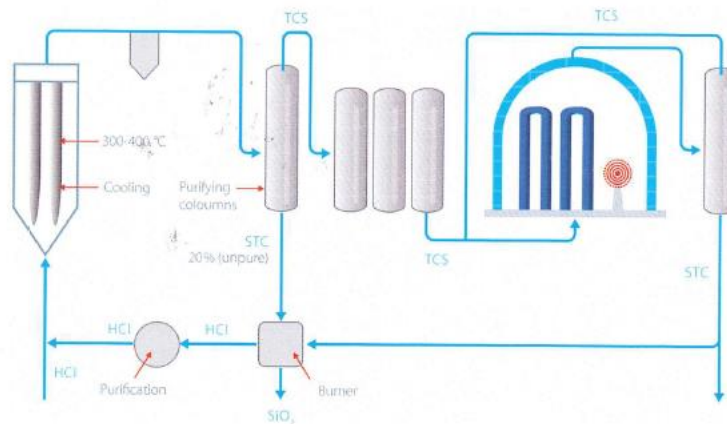


Figure 2.3: Siemens Process

The other route is the metallurgical route, and the chosen process in Norway. The metallurgical route can be simplified to three steps; slag treatment, leaching, and solidification [13]. As the same with the siemens process, MG-Si is the raw material used. The slag treatment is used to remove the boron for the MG-Si. In order to do this the MG-Si is melted down with a CaO-SiO<sub>2</sub> slag. Here the boron will react with the SiO<sub>2</sub> in the following reaction (5) and enter the slag phase.



Sometimes the leaching process is skipped and after the slag treatment the material is solidified. If leaching is necessary, the material is cooled and then crushed. The crushed material is treated with HCL and ferric chloride. What is left are silicon crystals 2 mm in size [12]. After leaching these crystals are re-melted and solidified into a larger block. The third step of solidification also acts as a treatment method. As the material is solidified, the impurities will stay in liquid form and can be removed easily.

Both of these methods have their advantaged and drawbacks. The Siemens process has a higher output than the metallurgical route. In 2011, the Siemens process produced 175,000 MT when the metallurgical route produced 35,000 MT. Even though the metallurgical route costs much less and uses less energy. The metallurgical route costs ~\$20/kg compared to the siemens process that can cost anywhere between \$25-\$45/kg. When looking at energy usage, consumption for the

metallurgical method is approximately 33 kWh per kilogram of silicon compared to 100-250 kWh for the siemens process [12]. Whichever method is chosen, both produce SoG-Si.

It is important to be aware of the three main types of solar cells being made; multicrystalline, monocrystalline, and thin-film. All three can be made with SoG-Si. Currently multicrystalline silicon is being produced at the highest rate of ~67%, monocrystalline at ~25%, and thin-film at ~8% as seen on figure 2.4 below [14]. The subsequent sections will look at monocrystalline and multicrystalline silicon. The post-treatment method will determine whether monocrystalline or multicrystalline is produced.

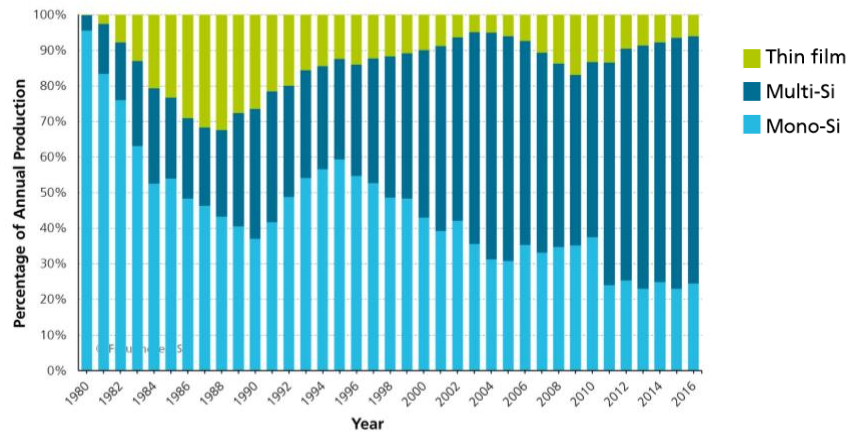


Figure 2.4: Production amounts for different solar silicon

Monocrystalline Si is produced through the well-established Czochralski process. This process was discovered in 1916 by Jan Czochralski [15]. With this process the SoG-Si is melted, and a seed crystal is dipped in the molten silicon. The seed crystal is slowly pulled up from the melt. The crystal being pulled up will have the same crystallographic orientation as the seed [16]. The rate that the crystal is pulled and cooled are closely monitored. The pulling process consists of different steps. First the “neck” of the crystal is created, the purpose of the neck is to remove defects that were formed from the temperature change of the seed being pulled from the molten metal. Next the crown is created to increase the diameter of the crystal. To help transitions, the shoulder is made next. This will help the crystal grow to its desired diameter. The different sections can be seen in the figure 2.5 below [16].

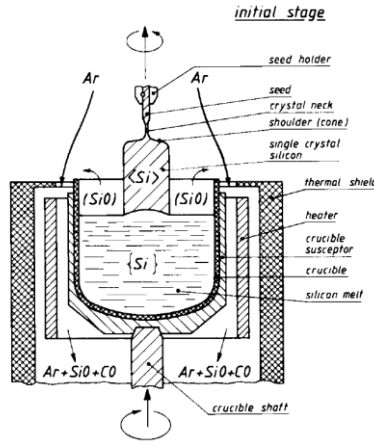


Figure 2.5: Schematic overview of the Czochralski process

Multicrystalline Si is produced through directional solidification. Here the SoG-Si is melted in a large carbon crucible. Once the SoG-Si is completely melted, the heat is removed, and the Si is cooled from the bottom up. The cooling rate is slow, usually around 10 mm/hour [16]. As the silicon is cooled the impurities, by means of segregation, will stay in liquid form and travel up to the top of the molten bath. This is better seen in the Scheil equation (eq 6)

$$C_S = k_0 C_0 (1 - f_S)^{(k_0 - 1)} \quad k_0 = \frac{C_S}{C_L} \quad (6)$$

This equation describes the concentration of the solute in the solidified part. We can see the concentration of the solute at the start of the cooling, when  $f_S = 0$ , is equal to  $k_0 C_0$ . As the ingot continues to cool, the amount of solute in the liquid will continue to rise. Once the material is fully solidified, all the impurities are located at the very top and can be easily cut off. It can easily be seen why multicrystalline SoG-Si is produced at more than double the rate of monocrystalline. Multicrystalline can be made in larger amounts in a shorter amount of time. Also, there is less operational man power needed for multicrystalline SoG-Si.

Impurities play an important role in the performance of solar cells, whether monocrystalline or multicrystalline. Impurities can either be introduced into the cell on purpose, known as doping, or they can be unwanted and introduced by the environment [17]. Some of the most common impurities found in the silicon are; oxygen, nitrogen, carbon, and iron. When impurities are in the metal they effect the efficiency by acting as traps and introducing energy levels in the band gap. There are a few different refining methods that can be used when the SoG-Si ingot is being produced. A popular method is by vacuum refining. Vacuum refining works when the dissolved

elements have a high vapor pressure and also a high segregation coefficient [18], [19] . The process is carried out by transferring the impurity from the melt to the gas phase.

Another factor to look at when comparing monocrystalline to multicrystalline is their respected efficiencies when they are manufactured into a solar cell. Because a monocrystalline solar cell is made from a single crystal, it should be no surprise that the monocrystalline cell outperforms the multicrystalline. A monocrystalline cell has a recorded efficiency of 26.7% while a multicrystalline cell has an efficiency of 22% [20]. The image below, figure 2.6, shows both monocrystalline and multicrystalline.



Figure 2.6: Monocrystalline ingot on the left and multicrystalline ingot on the right

## 2.2 Value chain of silicon production

The different steps of the value chain have been described in detail in the previous section and have been laid out in figure 2.7 below.

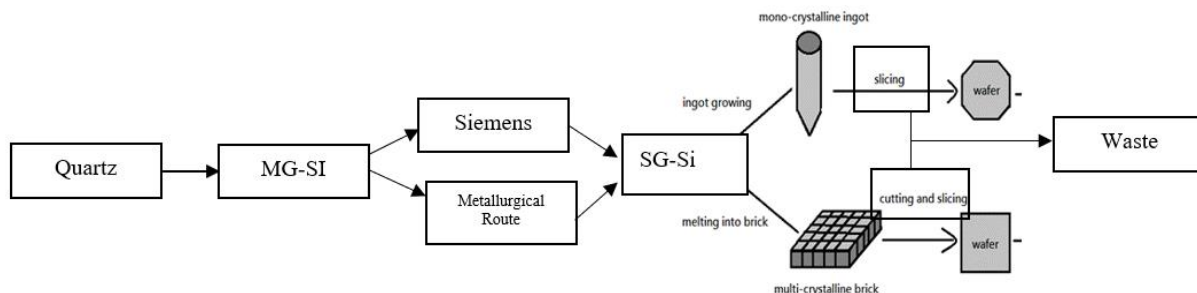


Figure 2.7: Value chain for solar silicon

The current value chain is mostly linear with a split when producing SoG-Si, whether the siemens process is used or the metallurgical route. There is also another split when it comes to what crystals are produced, monocrystalline or multicrystalline.

This project could redefine the current value chain to look something like this, figure 2.8, by taking the waste, agglomerating it, and recycling it back into the process.

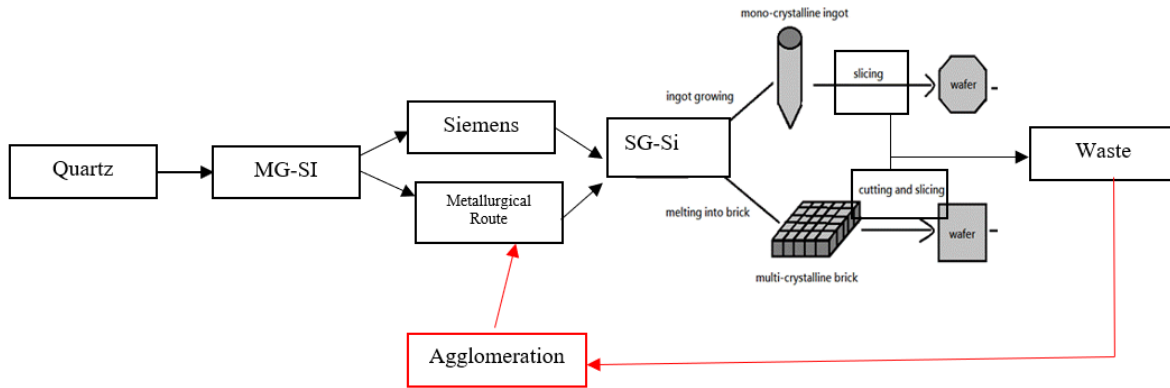


Figure 2.8: Proposed value chain

### 2.3 Cutting and wafering of solar silicon

The cutting and wafering of solar silicon contributes to 19% of the overall costs of production [21]. Before the ingot can be cut into wafers, it must be “squared” up. For a monocrystalline ingot, it is cut at the top and bottom to remove impurities and dislocations that may have formed during the pulling process. For a multicrystalline ingot it is first cut at the top to remove the high level of impurities that have gathered during directional solidification. It is then cut on all sides and the bottom. These areas are cut for any diffusion that might have taken place between the ingot and the crucible during the solidification process. These areas are known as the red zone and have mediocre electrical properties [16]. The biggest effect on this red zone is the quality of the crucible. As you increase the quality of the crucible, you will decrease the diffused impurity level and increase the lifetime. This zone can be seen when taking lifetime scans of the ingot as shown in figure 2.9.

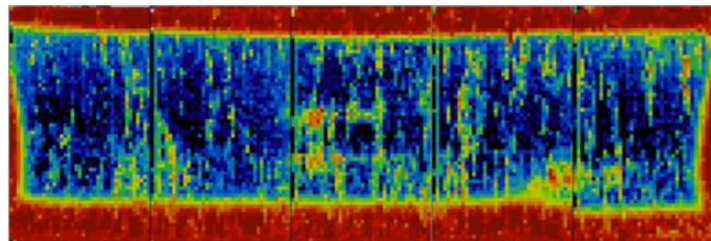


Figure 2.9: Lifetime map

As you move away from the edge of the silicon and towards the center, the color changes from red to blue. The red area denotes a low carrier lifetime while the blue area denotes a high carrier lifetime. After the ingot has been “squared” it can now be cut into wafers. The most common commercial sawing process to produce wafers is a multiwire saw. There are two methods with a multiwire saw, loose abrasive and fixed abrasive. A basic schematic of a multiwire saw is shown in figure 2.10 [22].

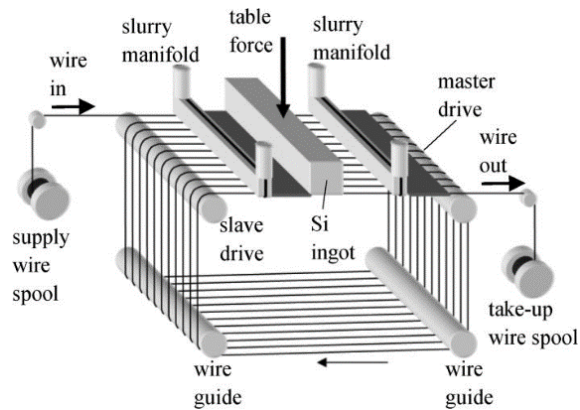


Figure 2.10: Multiwire saw

Even though it is known as a multiwire saw, it can be seen in the figure that the entire ingot is cut at once, using only one wire. The single wire makes it first pass at the front of the ingot and is further wrapped around rollers forming a wire “web”. Both methods use a wire with a diameter in the range of 80-120 $\mu\text{m}$  [21]. When a wafer is cut, it generally has a thickness somewhere between 100-200 $\mu\text{m}$ . For the loose abrasive method, a slurry made up of abrasive silicon carbide particles ( $\sim 4\mu\text{m}$ ) and polyethyleneglycol is passed over the ingot along with the wire. The friction created by the slurry is what cuts the ingot. When cutting with a fixed abrasive saw, the abrasive particles (typically in the form of diamond with a size of approximately 6-25 $\mu\text{m}$ ) are fixed directly onto the wire. As the wire passes over the ingot, the diamonds cut through. Many factors can lead to one method over the other, but the pros and cons have been summarized in the table 2.1 below.

Table 2.1: Comparison of sawing methods

<b>Method</b>	<b>Advantages</b>	<b>Disadvantages</b>
<b>Loose abrasive</b>	Variable thickness	Difficult to separate the slurry from the silicon kerf
<b>Fixed abrasive</b>	Thinner wafers	<ul style="list-style-type: none"> <li>• Coolant mixture is bad for the environment</li> <li>• Expensive to produce diamond wire</li> </ul>

## 2.4 Solar silicon waste

The thickness of the wafer is roughly the same size as the wire diameter, as the wire cuts through the silicon waste is produced during the wafering. During the wafering process, up to 40% of the total ingot is lost [9]. The other 10% of the ingot that is lost comes from squaring, cutting the top and sides of the ingot [9]. While half of the ingot is lost, currently the industry does not do much with this waste. The main challenge when dealing with this waste material is that it is combined with the slurry used from the abrasive saw. It is too much of a challenge to separate the high purity silicon particles from the small SiC particles. For every one tonne of ingot cut, six to seven tonne of slurry mix [21] is needed. As for how much waste is being produced annually, that number is a bit hard to find. In 2010, there was 101,750 tonnes of waste produced [9]. With the continued growth in the solar market, it can be assumed there will be growth in the waste being produced. As the waste continues to grow, this project becomes even more necessary.

## 2.5 Agglomeration theory and practice

### **History of agglomeration**

The idea of using fine grade low quality ore in the form of an agglomerate has been around since the 1900s. An agglomerate is the formation of fines into a bundle, and this idea has mainly been looked at with iron ore. Agglomeration started out with simple briquetting, but by the 1950s that was replaced with two other methods, sintering and pelletizing. The idea for agglomeration become so popular that in the 1960s, the United States alone was producing over 30 million tons of iron ore pellets [23]. The same methods that were used over 100 years ago are still being used today. This overview provides basic descriptions of briquetting, sintering, and provides the most detail on pelletizing of agglomeration.

After the end of the second world war, the global use of iron increased. Trying to keep up with this high demand, while also seeing a decrease in available raw material, forced producers to develop a new way to keep up with this newfound demand. Before these processes were developed, the producers would charge the blast furnace with lump ore while discarding the fine ore. Not using the fine ore resulted in the producers having growing piles of iron ore with no economic value. The fine ore was not suitable in the blast furnace because it would cause a drop in gas permeability and this drop would affect the desired performance of the blast furnace [24]. The small amount of fine iron ore that would find its way into the blast furnace was often blown out as flue dust and rendered as an economic lost to the producers. Producers in countries with low iron reserves were the first to start researching ways to reuse the flue dust by both briquetting and sintering. In countries with high iron reserves, this idea was not well received. As the demand for sintering the fines grew the need for a more consistent product was required. This created the foundation for the development of pelletizing the fine iron ore. Below is a brief summary of the three commercial methods used for agglomeration.

### **Briquetting**

The method of briquetting was the first agglomeration technique used and is the most basic. Fine ore particles are pressed together with a liquid binder under mechanical pressure, resulting in a briquet. While this method produces an excellent product, the cost and time involved can be too much to keep up with demand.

### **Sintering**

The method of sintering was originally performed on copper sulphide ores in the middle of the 19<sup>th</sup> century. Sintering was not used on iron ores until the 1950s. Sintering became popular over briquetting because it can be performed on coarser ore. The process of sintering consists of mixing the coarse ore with a form of coke and heating the mixture to slightly under the melting point of the ore. This heating causes the coarse ore to bond together, resulting in a sinter cake. The sinter cake is then further crushed into the desired size fraction. With this process, it can be hard to control the composition of the final crushed particles and their exact shape.

### **Pelletizing**

The method of pelletizing was developed as a way to utilize the fine ore particles that could not be sintered, and today is the method of choice for agglomeration. Fine ore is mixed with a binding material and rotated in a drum or disk. The process produces pellets with a uniform size distribution and even composition.

The three processes have been summarized in the table 2.2 below

Table 2.2: Comparison of size and shape for three agglomeration processes

Method	Briquetting	Sintering	Pelletizing
Size	~3cm	5-50mm	9-15mm (diameter)
Image			

## 2.6 Pelletizing principles

As the demand grew for a way to use this previously unusable material, a new method was developed, pelletizing the fine ore. By pelletizing the fine ore, they were able to make a more consistent product in a shorter amount of time. The first countries to really pave the way for pelletizing were Sweden and Germany [24]. Sweden, in their testing, was the first to find that these pellets could be produced faster than the sinter product in the furnace. Even with this discovery, pelletizing in Europe was not able to compete with the sintering process and was abandoned. The next big development in the pelletizing process took place on the “Iron Range” of Minnesota. Here it was discovered that ore fines that were too small to be sintered could be pelletized instead. As news of this new discovery spread to Europe, pelletizing research was reborn. As pelletizing was being researched again in Europe, it was discovered that as the size of the fines decrease so does the sintering production. This can be seen in figure 2.11 [24] below:

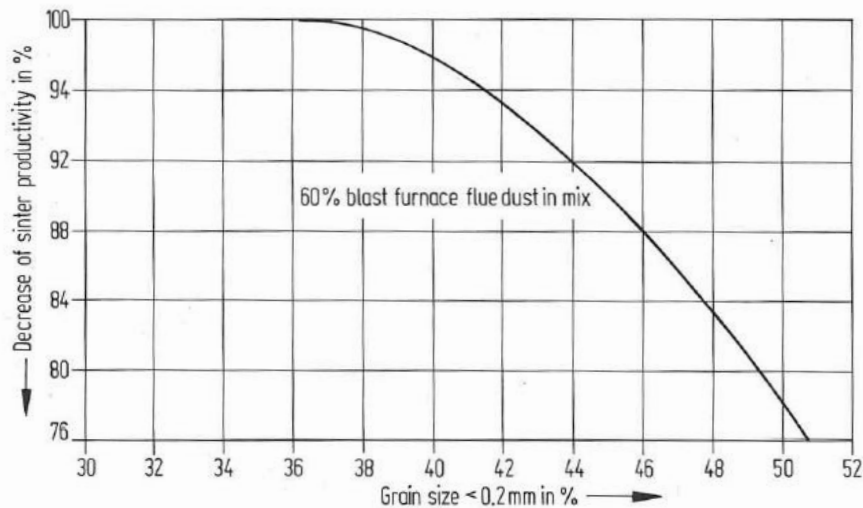


Figure 2.11: Sintering productivity in relation to grain size

This new discovery helped increase the popularity of pellets and the increase in the production of pellets as seen in figure 2.12 [24].

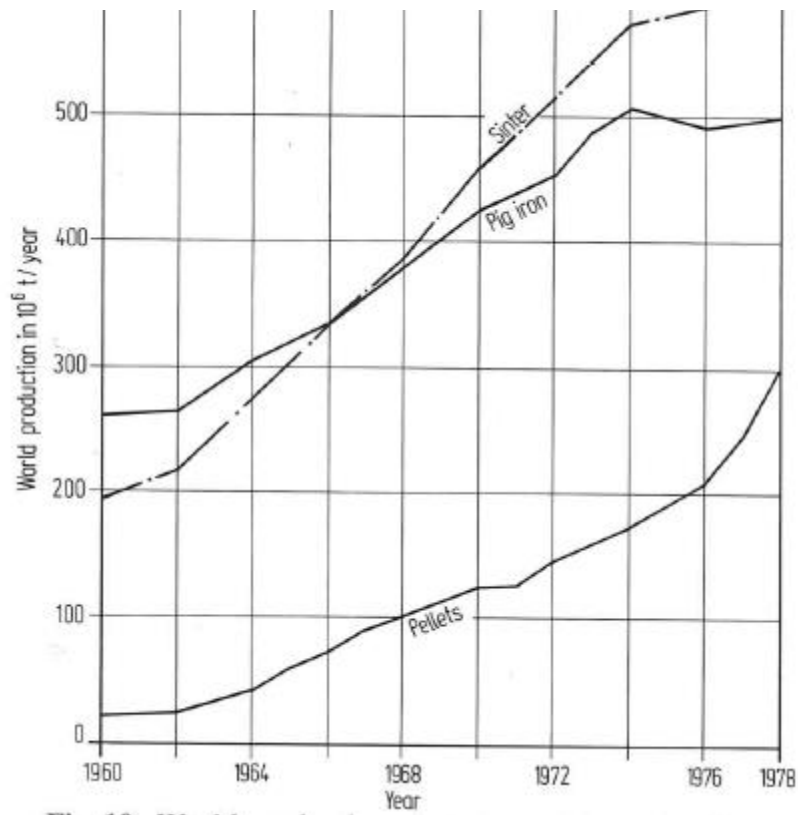


Figure 2.12: Increase in a production of pellets over time

### Pelletizing Process

The process for creating pellets can be done in three basic steps; material preparation, formation of green balls, and heat treatment of green balls [24]. The process of material preparation is simple, here the ore is crushed and sized for the optimal distribution. During green ball formation, the material is combined with a liquid binding agent and mixed in a drum or disk. There are many different factors in the formation step that can affect this process. During this step, the binder plays a key role in the green ball formation. Trying to choose the right binder is one of the most important process steps in the pelletizing process. There are three main reasons to use a binder; to help achieve the correct green strength, to help achieve the correct dried strength, and to contribute in the actual pelletizing process [25]. When the binder is used to contribute in the pelletizing process, it holds the fine particles together through capillary forces, seen in figure 2.13 [24]. If too much binder is added, the capillary forces will no longer be present and can turn the material into a paste [24].

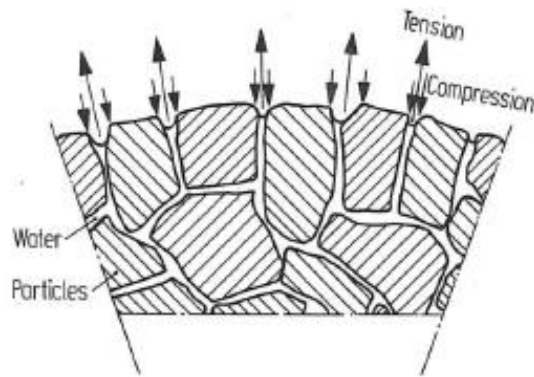


Figure 2.13: Capillary forces on green balls

Each ore will have its own shape and size distribution and will require an investigation to figure out the right parameters for green ball formation. The green balls have a mechanical strength too low to be used directly after their formation and must be heat treated. There are tests that can be done to the green balls to check for quality. Some of these tests are; moisture content, crushing strength, drop number, and drop resistance. When the green balls have passed these tests, it is time for them to be dried and then fired. There are three commercial furnaces that will dry and fire the green balls. The three different furnaces are a shaft furnace, grate-kiln, and a straight grate [11]. Each of these has its pros and cons and the parameters and quality of the desired pellets will dictate which furnace will be used. During the drying stage, the process is non-linear and slows down over time. If the green ball is dried too quickly, it can lead to cracking or splintering. Once the pellet is dried it is transported to be fired. During the firing, the pellet is heated to an optimal temperature for the specific material. This temperature is below the melting point, but in the reactivity range of the unwanted components within in the pellet. As the pellet is being fired, the individual lattices undergo diffusions and re-arrangements which leads to re-crystallization of the grains [24]. After this re-crystallization process is finished. The final step in the pellet production process is the cooling. The pellets cannot be cooled too fast or they will be at risk for damaging the crystallization that took place in the heat treatment. Most studies show that the pellets must be cooled in air to 300 degrees Celsius before being quenched in water to avoid damage [24]. Just like with green balls, the heat-treated pellets must be tested. Some of the tests performed on them are; crushing strength, tumbler resistance, and microporosity.

While there may seem to be several steps involved in pelletizing when taking into account decisions on the correct furnaces to use, the testing that is completed during the green ball formation, and after heat treating, it has become the method of choice. It is ideal for fine ore particles. As indicated previously, it results in pellets of uniform size distribution and even composition in the shortest amount of time.

### 3 Experimental procedure

The applied methodology in the present research is described as follows

#### 3.1 Characterization of silicon fine powder

The fine silicon material for this project were provided by REC Solar, and needed to be characterized. To characterize the silicon fine material four different tests were carried out; X-Ray Diffraction (XRD), Scanning Electron Microscopy (SEM), Inductively coupled plasma mass spectrometry (ICP-MS), and particle size analysis. The XRD measurements were conducted in the 2 theta range from 20-80 degrees with a 0.03 step. The particle size distribution was measured by Horiba laser particle size analyser. The powder (~5mg) was added to 50mL of isopropyl alcohol and run through the machine two times. SEM analysis was done to study the morphology and also the particle size of the silicon particles. This was carried out on a Ziess ultra 55 model. The ICP-MS was done across three parallels. In order to do ICP-MS, the sample must be in the form of a liquid solution. In order to prepare the solution, the silicon fines were digested in a combination of nitric and hydrofluoric acid.

#### 3.2 Characterization of microsilica

The microsilica, which was also provided by REC Solar, needed to be analysed as well. To analyze this material, three tests were conducted; XRD, SEM, and particle size analysis. The XRD measurements for the microsilica were conducted in the same manner as the silicon fines, in the 2 theta range from 20-80 degrees with a 0.03 step. To measure the particle size, the microsilica was added to 50mL of isopropyl alcohol and run through the machine three times. To confirm the morphology and size, SEM was carried out on the microsilica using the same Ziess ultra 55 model.



Figure 3.1: Material provided by REC Solar, silicon fines on left, microsilica on right

### 3.3 Making agglomerates by press

In order to make silicon agglomerates in the lab, compressed pellets were made, which is a methodology to show the potential of applying both briquetting and pelletizing techniques. In this case, briquettes were formed by uniaxial pressing, as shown schematically in Figure 3.2 [26].

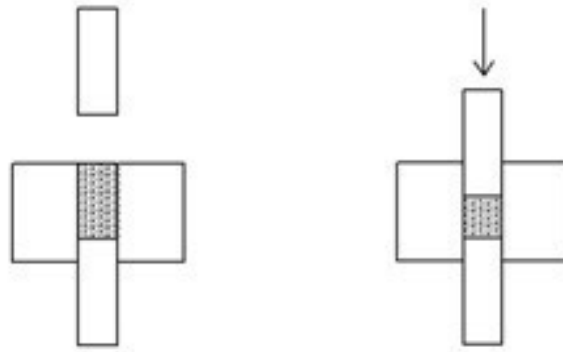


Figure 3.2: Uniaxial press schematic

In order to make the briquettes, batches of 20 grams of silicon powder was mixed with water in four different amounts of 0, 3, 6 and 10 wt%. The powders were mixed in a make-shift ball mill fashion. 22 steel balls (54g) with a diameter of 0.5cm were added to the water and powder mixture to help with a more uniform mixing, as seen in figure 3.3.



Figure 3.3: Mixing the combination of water and silicon fines with the use of steel balls

All of the briquettes that were pressed had a diameter of 10mm and were pressed with 800kg of force. Moreover, in order to study the effect of the applied load in pressing, some samples were pressed with 400kg and 1200kg from a powder mixture that contained 10 wt% water. Briquettes that had a diameter of 10mm and a height of 10mm were made with 1 gram of the powder mixture.



Figure 3.4: Hand press that was used to produce the briquettes

### 3.4 Making briquettes with binders by press

Along with water, three different binders were added to the fine silicon powder and pressed into briquettes as well. The binders that were used were microsilica (a by-product of the silicon process), hydrated lime, and an organic binder. These briquettes were made in the same fashion as the briquettes in the previous section. 20 grams of fine silicon powder was mixed with binders in three different amounts; 2, 4, and 6 wt%. After the powders were mixed, a constant amount of 10 wt% water was used. The powders were mixed in the same “ball mill” fashion and the briquettes were pressed with a constant load of 800kg. A summary of the briquettes that were produced is in the table 3.1 below

Table 3.1: Summary of briquettes made with binder

<b>Binder Type</b>	<b>% Binder</b>	<b>% Water</b>
Organic Binder	2	10
Organic Binder	4	10
Organic Binder	6	10
Microsilica	2	10
Microsilica	4	10
Microsilica	6	10
Hydrated lime	2	10
Hydrated lime	4	10
Hydrated lime	6	10

### 3.5 Strength test for green briquettes

In order to evaluate the strength of the briquettes, a drop test was designed. Currently there is no method to evaluate silicon agglomerates. The standard method for iron pellets is to drop test them from a height of 46cm onto a steel plate [7]. After discussions with industry, a test method was designed to drop the pellets from a height of 23cm onto a steel plate. A lesser height was chosen, because the agglomerates will be manufactured on site. After the briquettes were pressed, they were dropped in the longitudinal direction from a height of 23cm onto a steel plate. The number of drops till they first broke and the number of drops until they shattered were recorded. The Shatter number is actually the number of drops until the briquette is broken to sizes below 50% of briquette's volume; this means the biggest broken part is smaller than half of the initial volume. For instance, if the briquette is getting smaller and smaller in the drop tests, and at drop 16 it is still larger than half of the initial briquette, and it is then broken in drop 17 to several particles and the biggest one is smaller than the half of the initial briquette, the drop number is recorded as 17.

### 3.6 Induration of green briquettes

Induration plays an important role in the agglomeration process, by indurating the briquettes they take on their final hardened form [agglomeration handbook]. An indurated agglomerate strength is important for this process, because it must withstand being charged in the furnace without breaking up [24]. Induration was done at different temperatures to see its effect on the briquettes. It was first done on briquettes made with 2 wt% organic binder with 10 wt% water, these briquettes were dried in 60° C, and were looked at four different times. This temperature is below the melting

point of the organic binder. Briquettes were dried for 30, 60, 120, 180 minutes. The briquettes were weighted before they were put in the oven and weighed again after they were taken out. Next briquettes were indurated at temperatures about the melting point of the organic binder at 80° C. The briquettes that were indurated at this temperature contained 2 wt%, 4 wt% and 6 wt% binder. All of these briquettes also contained 10% water. The briquettes were once again dried for 30, 60, 120, 180 minutes. The briquettes that contained 2 wt% binder were weighted before they were put in the oven and weighed again after they were taken out.

### 3.7 Strength test for indurated briquettes

The same strength test that was used for the green briquettes was used for the indurated briquettes, the drop number test. The briquettes were dropped from a height of 23cm onto a steel plate. It was recorded when the briquettes first broke and when they shattered.

### 3.8 Making agglomerates by pelletizing

In order to make pellets, a pelletizing disk was used and can be seen in figure 3.5 below. A single batch of material was made and run through the disk. The batch of material totaled 850 grams with 6 wt % of that being the organic binder and the rest the silicon powder. The water content that was mixed into the powder mixture was 10%. It should be noted that extra water was misted into the drum as the material was being pelletized. The pelletizing disk, as seen in figure 3.5, produced two sizes of pellets; pellets that were larger than 4.5mm and pellets there were larger than 1.8mm but smaller than 4.5mm.



Figure 3.5: Pelletizing Disk

### 3.9 Induration of green pellets

After the pellets were separated into their two size fractions, they were indurated in an oven. The pellets were dried for 5 hours and at a temperature of 80° C. The group of pellets were both weighted before they were put in the oven and after they were taken out of the oven.

### 3.10 Strength test for pellets

A sample of pellets were tested for the green strength and also their indurated strength. In the same fashion as the briquettes, the pellets were tested the same way. Both green pellets and indurated pellets were dropped from a height of 23 cm and onto a steel plate. When the pellets first broke and when they shattered were recorded.

## 4 Results and Discussion

The results about the characteristics of the silicon particles, microsilicon particles, and their agglomeration behaviour are presented as follows.

### 4.1 Characteristics of silicon particles

In reviewing all the tests that were done to characterize the material, the results from the XRD are shown in figure 4.1. From the figure 4.1, one can see that the material aligns with crystalline silicon. In figure 4.1, the standards are shown as red lines and the measured counts are denoted as black peaks. All the standards are located inside the peaks, this indicates the material is crystalline silicon. The size analysis reports an average size of  $9.34\mu\text{m}$  and the full curve is shown in figure 4.2. The distributions of both tests that were run can be seen, and both tests have nice results and follow the same shape. The material has an overall nice distribution that will be good for both briquetting and pelletizing, the material is too fine for sintering [7]. From the SEM figure 4.3, one sees that the material has nice uniform morphology and is not amorphous. The sizes of the particles can be seen in the SEM images and also confirms the results that were seen from the particle size analyser. ICP-MS was also done on the sample and the results are shown on table 4.1 below. The table shows that three samples have red values (Ba, P, and Ti). The samples are in red because of their high relative standard deviation (rsd) with their rsd in parentheses. It makes sense to see a high error value, because there is less of the Phosphorus in the sample; it is harder to get an accurate reading. One can see this as well with the Ba and Ti, the amounts in the sample are low, leading to a high chance of error. We know that phosphorus has a huge effect on the performance of the cell, as discussed in the previous sections, so it is a disappointment that the margin of error is so high for that element. The other two elements in high amounts, but with acceptable rsd are Al and Ca. At the amounts of these two elements in the silicon, it can lead to issues with the overall performance of the cell.

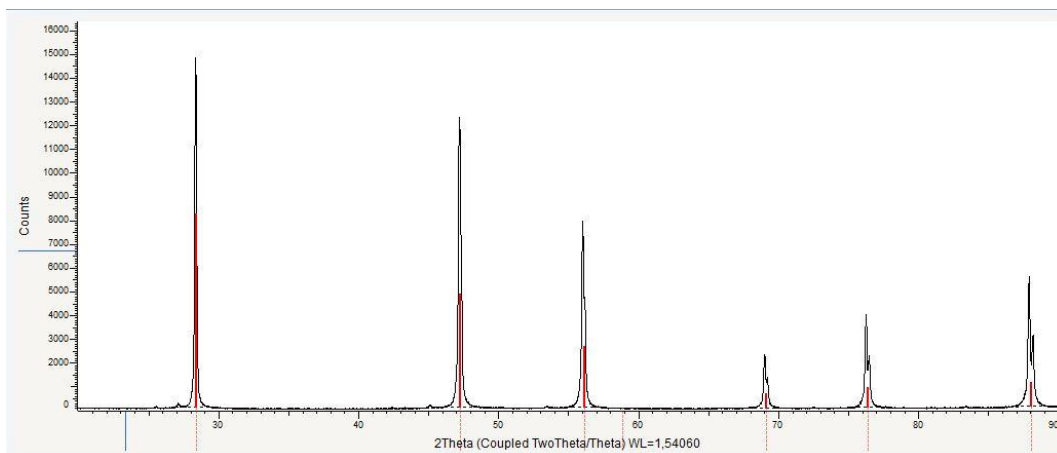


Figure 4.1: XRD mapping of silicon

# HORIBA Laser Scattering Particle Size Distribution Analyzer LA-960

Batch	: Si sample 1	Treatment	:	Median size	:	7.19470 (µm)
ID#	: 201709261031974	Operator	: Matthew	Mean size	:	9.34234 (µm)
Data name	: Test1-ultrasound1	Source	: Elkem	St. Dev.	:	9.3610 (µm)
Transmittance (R)	: 47.2 (%)			Geo. mean size	:	6.3928 (µm)
Transmittance (B)	: 46.3 (%)			Geo. St. Dev.	:	2.5168 (µm)
Circulation speed	: 10			Mode size	:	9.4151 (µm)
Agitation speed	: 4			Span	:	Off
Ultrasound	: 01:00 (7)			Diameter on cumulative %	:	(2)10.00 (%) - 1.8028 (µm)
Iteration mode	: Manual					
Distribution base	: Volume					
Refractive index (R)	: Si in isopropanol [silicon(3.500 - 0.000i),isopropanol(1.378)]					
Refractive index (B)	: Si in isopropanol [silicon(3.500 - 0.000i),isopropanol(1.378)]					
Material	: Si 99%					□

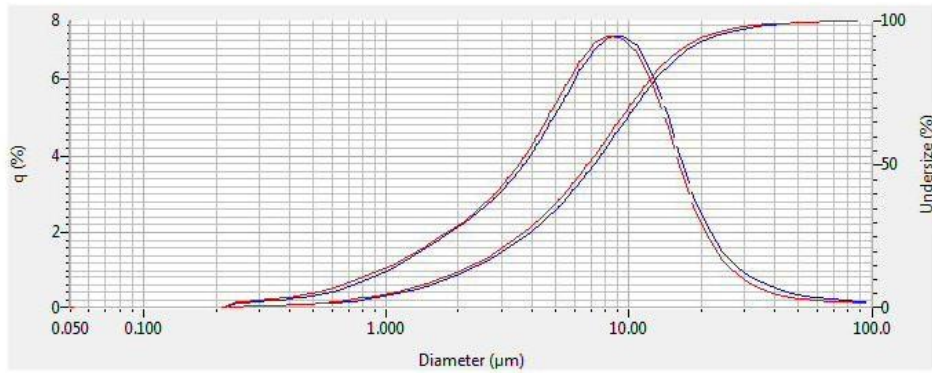


Figure 4.2: Particle size distribution of the fine silicon

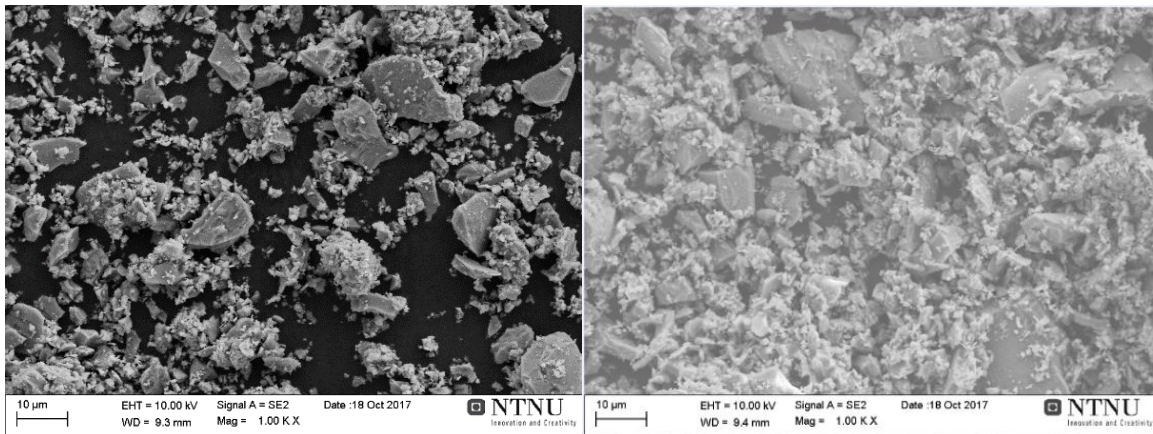


Figure 4.3: SEM of the fine silicon

Table 4.1: ICP-MS results for silicon

<b>Element</b>	<b>Ppm</b>
Aluminum	178.49
Boron	5.82
Barium	1.321 (28.7)
Calcium	265.6
Cobalt	40.013
Chromium	2.49
Iron	84.57
Magnesium	4.2
Manganese	1.486
Nickel	2.15
Phosphorus	2.14 (10.5)
Titanium	4.35 (16.2)
Zirconium	0.213

## 4.2 Characteristics of microsilica particles

The first test that was done to the material was XRD, and the results can be seen below in figure 4.4. One can see that unlike the XRD for the silicon (figure 4.1) we do not get nice uniform peaks. This was a bit expected, because the microsilica is amorphous in crystalline structure. Because the microsilica is amorphous in nature, it is not surprising that it does not line up with the peaks as we saw for the silicon fines. The next test carried out was the particle size analysis. A wet test was run and the distribution is shown in figure 4.5 below. The test was run three times and looking at the figure, it can be seen that each time the test was run, a different distribution was produced. When looking at the figure the average size is ~20  $\mu\text{m}$ . When comparing that to the silicon, in the section above, the average size is twice as large. This is most likely the result of an error during the measuring process. The last test that was run on the material was SEM, images were taken at both the micro-level and also the nano-level. Looking at the image that was taken at the micro-level, figure 4.6, the particles are uniform in size and shape. It can be seen from the SEM that the size of particles does not match what was read from the particles size analysis. The shape of the particles is more or less spherical, that is expected. When zooming in on the particles and looking at them on the nano-scale, figure 4.6, one can see that the overall particle is actually made up of nano particles. Once again, this is expected as the microsilica is formed through condensation during the production process.

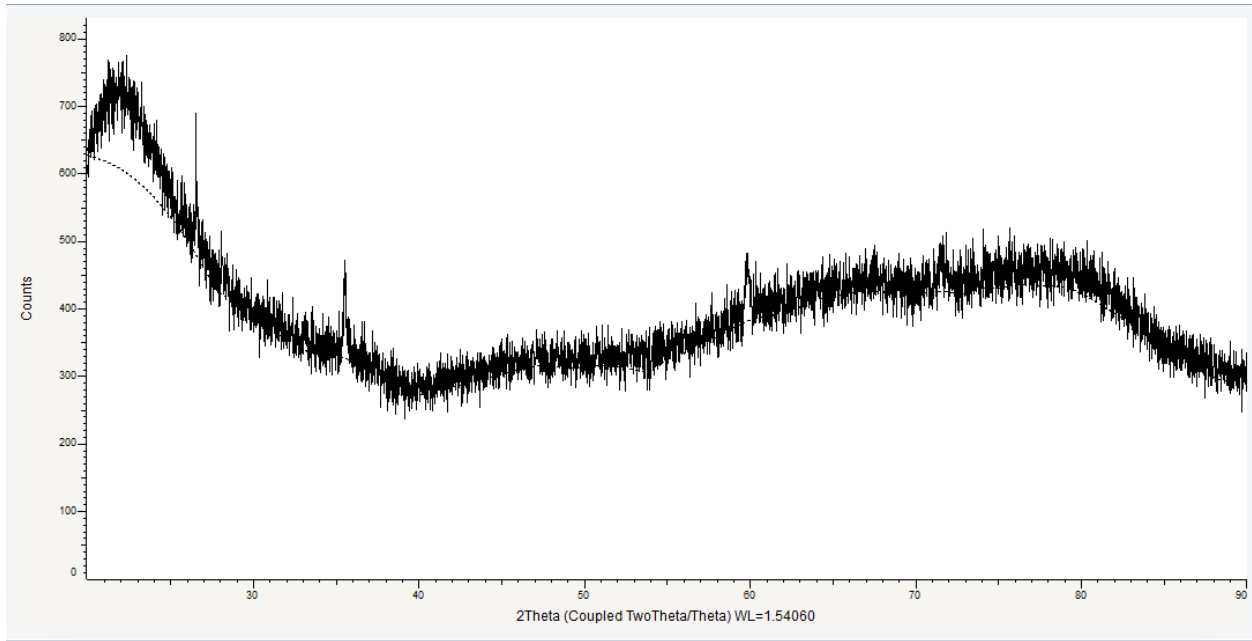


Figure 4.4: XRD mapping of microsilia

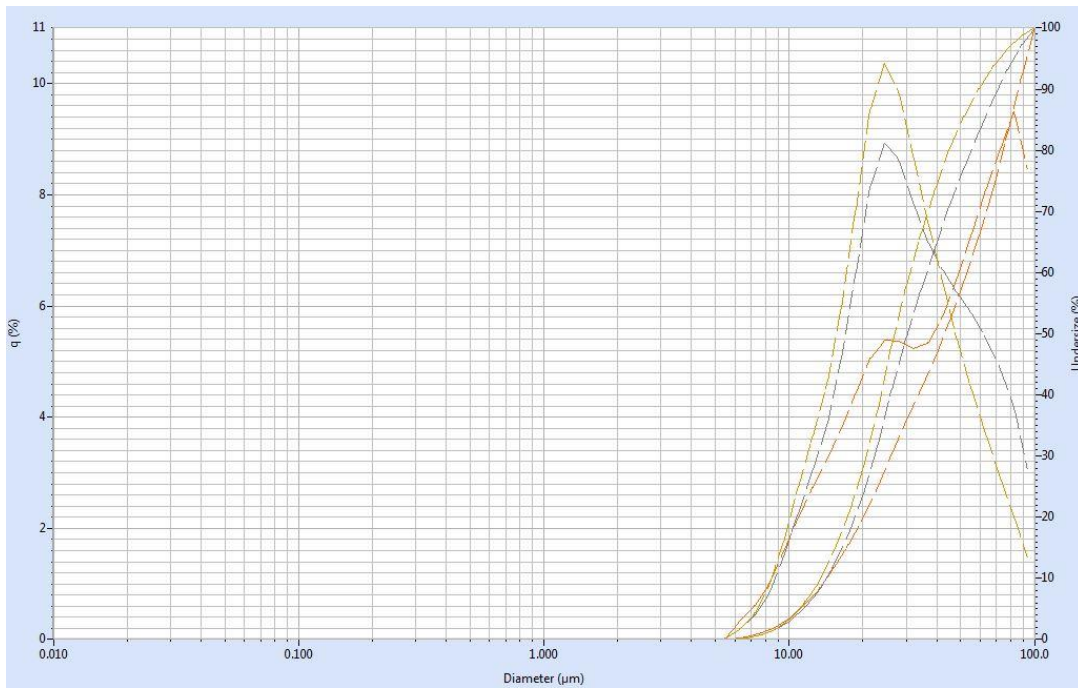


Figure 4.5: Particle size distribution of the microsilia

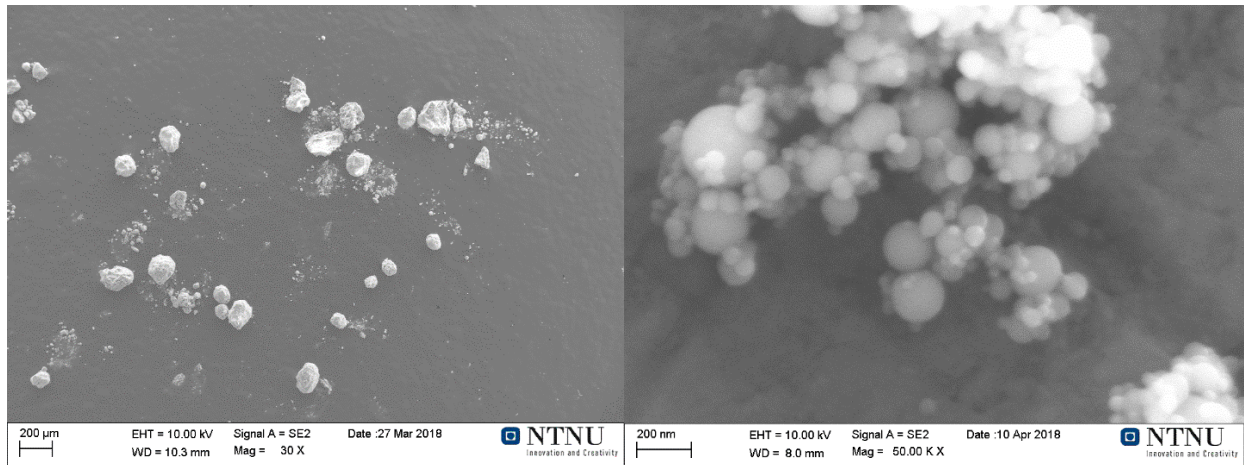


Figure 4.6: SEM of microsilia

### 4.3 Strength of green briquettes

An important parameter of the agglomerates are their properties before they are indurated at elevated temperatures. A pre-heat-treated agglomerate is known as a “green” agglomerate, and the properties of these green agglomerates are important. The strength is the most important property of the pre-indurated agglomerate, which is usually evaluated by the drop number. The drop number indicates how many times the green agglomerate can be dropped before they crumble [7]. This property is important because the pellets must be able to survive all of its post production handling without breaking. To find the drop number, the briquettes were dropped from a height of 23cm onto a steel plate.

A methodology was applied for the first time in this study in which single briquettes were dropped from a height of 23cm on to a steel plate. The drop number after their first break was noted and the drop number when the pellet shattered (more than 50% breakage) was noted. The obtained numbers for three single pellets of each moisturized silicon-water mixture are presented in Table 4.2.

Table 4.2: Drop test results for green briquettes made with water

Wt % water	1 <sup>st</sup> break	Shatter
0	1	1
0	1	1
0	1	1
3	1	17
3	1	18
3	1	25
6	1	19
6	1	15
6	1	21
10	2	16
10	6	17
10	6	26

The first break for the first nine briquettes all had the same results, occurring on the first drop. While the briquettes that were made with zero water did not survive any of the drops, the 1<sup>st</sup> break number for the briquettes that were pressed with water was most likely from an error in the pressing.

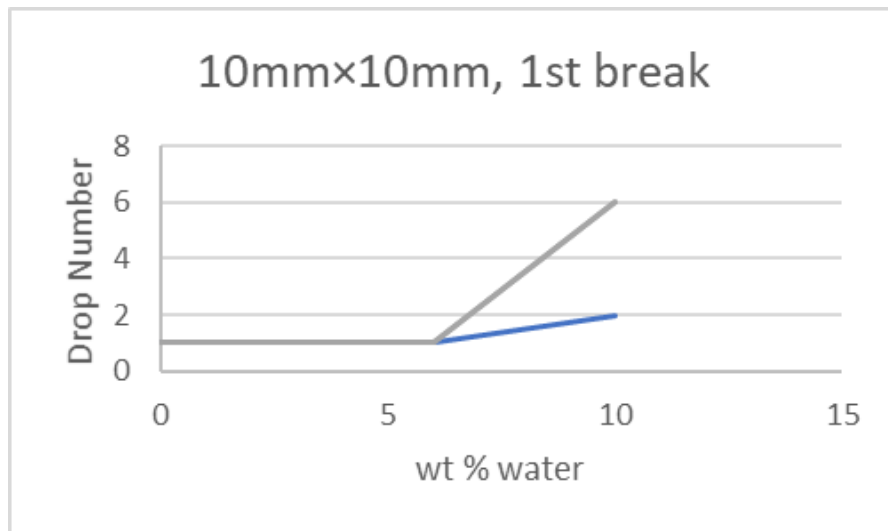


Figure 4.7: First break number of green briquettes

When all of the first nine briquettes were pressed, a “lip” was formed on the bottom, shown in figure 4.8. When the briquettes were dropped, this “lip” was the first thing to break off. When the “lip” broke off, it can be seen in figure 4.8 that this “lip” broke off intact in one piece.

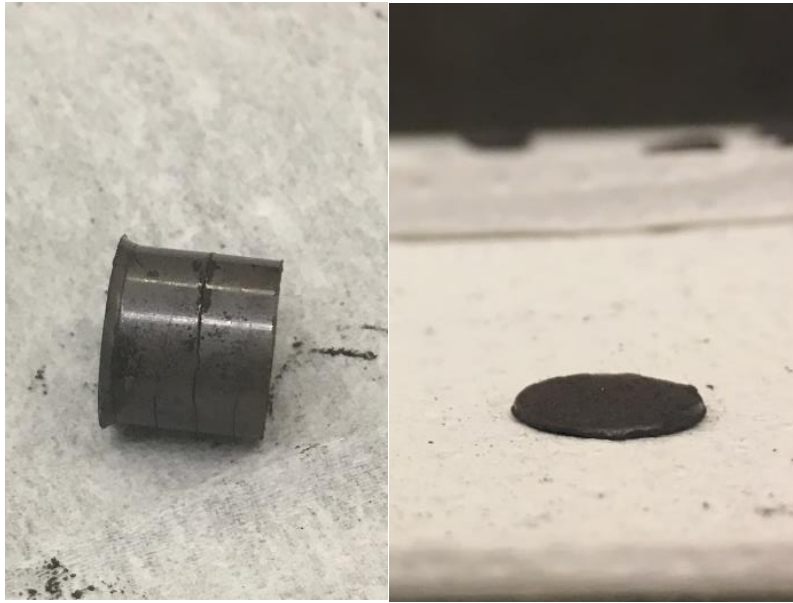


Figure 4.8: Press error, “lip” formed on the left, and broken “lip” on the right

When looking at the graph for the shatter number seen below in figure 4.9, things are a little clearer.

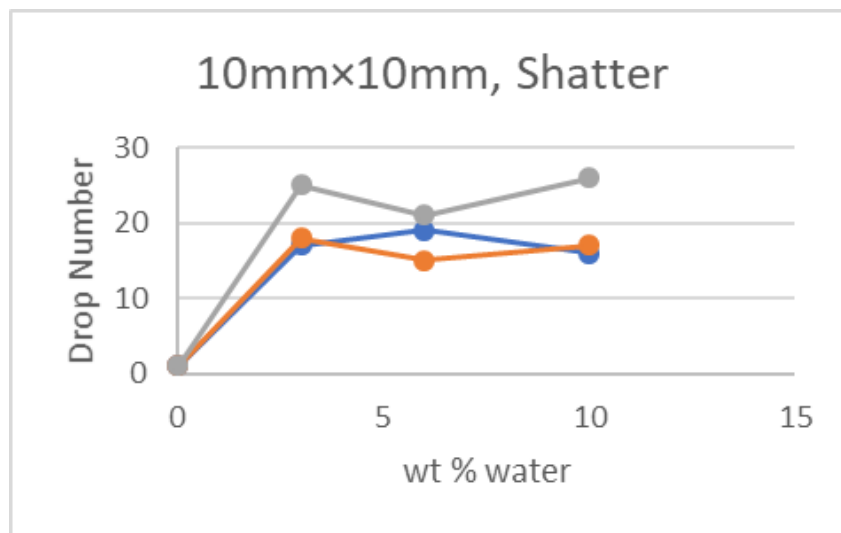


Figure 4.9: Shatter number of green pellets.

With these briquettes as the water content was increased the shatter number also increases. It can be seen that here the water amount does not have that much influence on the shatter number, as all sets of pellets performed about the same. It is interesting to notice that as the amount of water was increased in a linear manner that the drop number did not performed in the same linear rise.

When we look at the effect that the applied load has on the strength of the briquettes as seen in figure 4.10. It can be seen that the briquettes pressed with the load of 800 kg had a higher shatter number than the briquettes pressed with both the 400 kg load and the 1200 kg load

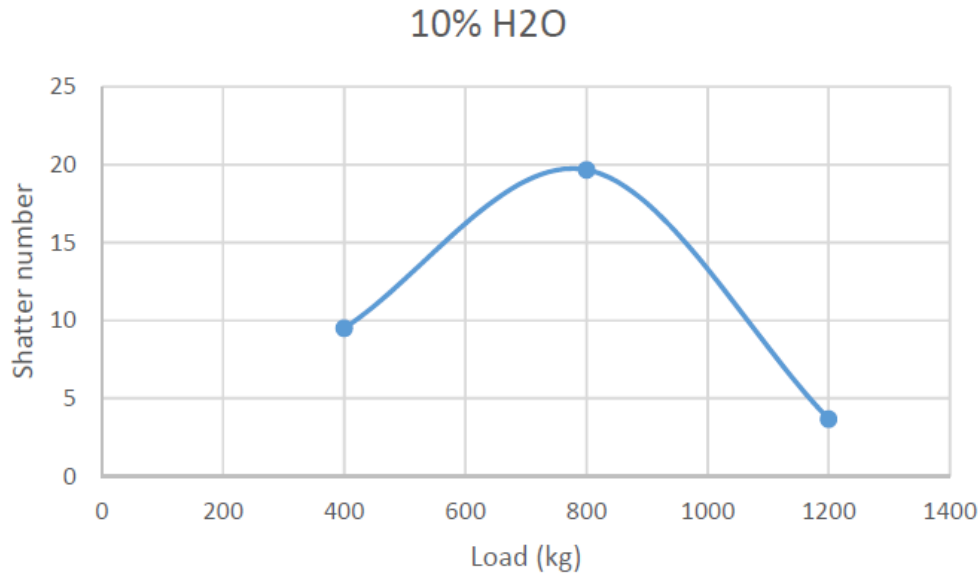


Figure 4.10: Shatter number with varied applied load

#### 4.4 Strength of green briquettes with binder

To see what effect the binders had on the briquettes, three different binders in three different amounts were produced as we see in table 4.3. These briquettes were evaluated for their first break and when they shattered. The results to these tests are shown on table 4.3 below. The graphs seen below in figure 4.11 and figure 4.12 are the averages of the briquettes performance.

Table 4.3: Drop test results for green briquettes made with binder

<b>Binder Type</b>	<b>% Binder</b>	<b>1<sup>st</sup> break</b>	<b>Shatter</b>
Organic Binder	2	7	25
Organic Binder	2	13	19
Organic Binder	2	10	35
Organic Binder	4	3	18
Organic Binder	4	6	11
Organic Binder	4	13	22
Organic Binder	6	6	23
Organic Binder	6	7	18
Organic Binder	6	11	14
<b>Binder Type</b>	<b>% Binder</b>	<b>1<sup>st</sup> break</b>	<b>Shatter</b>
Microsilica	2	3	18
Microsilica	2	3	20
Microsilica	2	6	16
Microsilica	4	4	16
Microsilica	4	4	22
Microsilica	4	5	24
Microsilica	6	1	22
Microsilica	6	3	14
Microsilica	6	9	12
<b>Binder Type</b>	<b>% Binder</b>	<b>1<sup>st</sup> break</b>	<b>Shatter</b>
Hydrated Lime	2	5	15
Hydrated Lime	2	7	17
Hydrated Lime	2	8	21
Hydrated Lime	4	4	16
Hydrated Lime	4	6	18
Hydrated Lime	4	6	24
Hydrated Lime	6	5	21
Hydrated Lime	6	9	17
Hydrated Lime	6	11	23

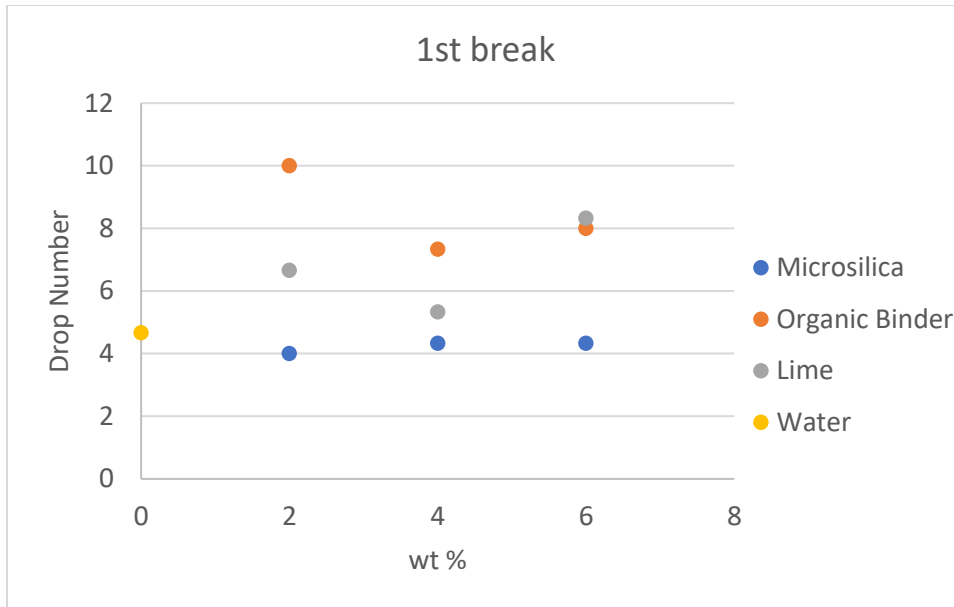


Figure 4.11: First break number of green briquettes with binder

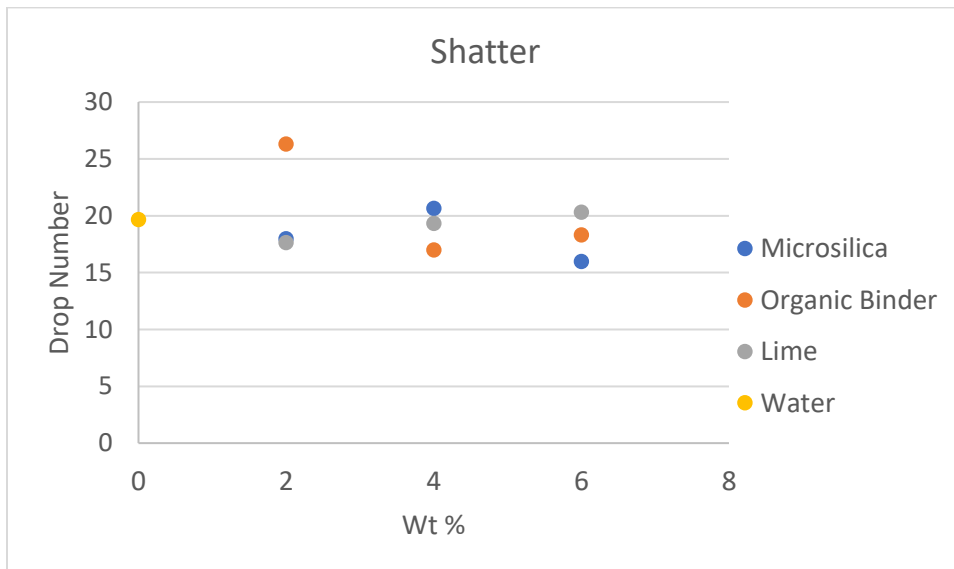


Figure 4.12: Shatter number of green briquettes with binder

When looking at the graphs, one sees on the y-axis a single dot. That dot is a briquette made without any binder, only 10 wt% water. The value for that has come from the average of the previous test seen in table 4.2. It is once again interesting to see that the increased binder amount does not mean an increased performance. Both graphs show, that with each different binder, no matter the amount, they performed about the same. The data also shows that by adding a binder to the briquettes does not mean an automatic superior product when comparing it to using only water. When looking at the microsilica, one sees that that was just the opposite. When microsilica was added as a binder to the briquettes, the performance was worse than just using water.

#### 4.5 Strength of indurated briquettes

Before looking at the strength of the indurated pellets, it is important to understand what is happening to these briquettes as they are dried. To see how the briquettes react to the oven, each briquette was weighed before and after being in the oven. The briquettes were indurated at two different temperatures. Looking first at the briquettes that were indurated at 60°, the results can be seen in table 4.4 below:

Table 4.4: Mass loss of briquettes dried at 60°

Binder	% Binder	% Water	Drying time	Drying temp	Mass loss (%)
Organic Binder	2	10	30min	60	4.8
Organic Binder	2	10	60min	60	5.8
Organic Binder	2	10	120min	60	6.3
Organic Binder	2	10	180min	60	4.6
None	N/A	10	30min	60	3.1
None	N/A	10	60min	60	5
None	N/A	10	120min	60	7.2
None	N/A	10	180min	60	5.4

The table shows the important data, consisting of the drying temperature and mass lost. It is important to remember that the drying temperature was below the melting point of the organic binder. Because the drying temperature is below the melting point of the binder, we can expect to see the drying just effecting the water in the briquette. This is confirmed in the table above as the briquettes were in the oven, whether they had binder or just water, the mass loss was essentially the same.

After the briquettes were taken out of the oven they were evaluated for their drop number, when they first broke and when they shattered

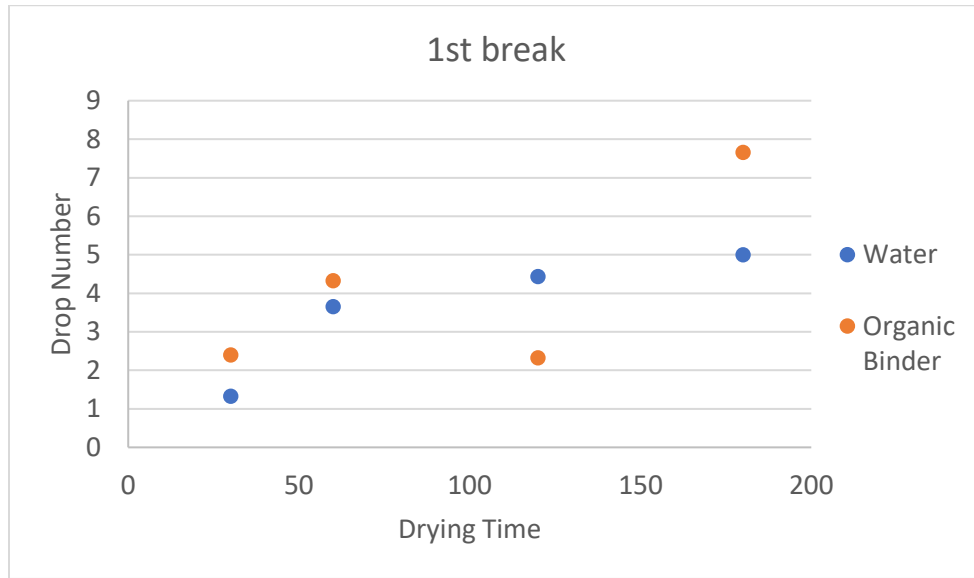


Figure 4.13: Comparison of briquettes, water vs organic binder, dried at 60°, first break

When looking at when the briquettes first broke in the graph above, figure 4.13, one sees that the longer they were in the oven the better they performed. As the drying time increased so did the drop number. It is interesting to note that when looking at the shatter number, in the graph below, figure 4.14, the same trend, as the drying time increases, the shatter number increases. The data also shows that when it came to the shatter number, the briquettes with only water outperformed the briquettes with the binder. This is a switch from the 1<sup>st</sup> break number where the binder briquettes outperformed the briquettes with just water.

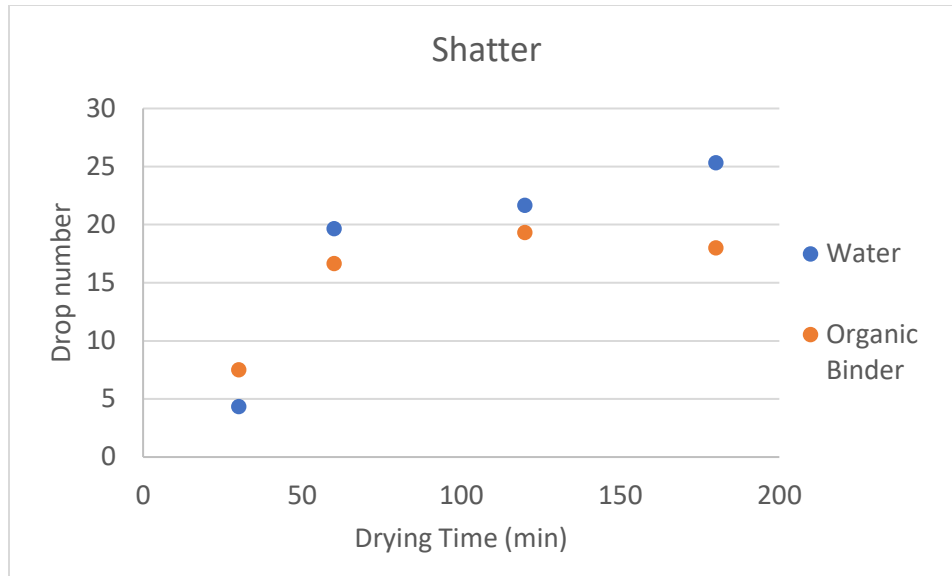


Figure 4.14: Comparison of briquettes, water vs organic binder, dried at 60°, shatter

To determine how the briquettes will perform when they are indurated at temperatures above the melting point of the binder, and also with the binders in different amounts, briquettes were made and dried at 80°.

Table 4.5: Mass loss of briquettes dried at 80°

Binder	% Binder	% Water	Drying time	Drying temp	Mass loss %
Organic Binder	2	10	30	80	5.6
Organic Binder	2	10	60	80	4.8
Organic Binder	2	10	120	80	8
Organic Binder	2	10	180	80	11
Organic Binder	4	10	30	80	3
Organic Binder	4	10	60	80	N/A
Organic Binder	4	10	120	80	N/A
Organic Binder	4	10	180	80	N/A
Organic Binder	6	10	30	80	N/A
Organic Binder	6	10	60	80	N/A
Organic Binder	6	10	120	80	N/A
Organic Binder	6	10	180	80	N/A
None	N/A	10	30	80	4
None	N/A	10	60	80	4.8
None	N/A	10	120	80	5.7
None	N/A	10	180	80	5.4

The mass loss of the briquettes is shown in the table 4.5. Here is it important to remember that these briquettes were dried at temperatures above the melting point of the organic binder. In the table 4.5, it can be see that the briquettes with only water had a constant mass loss and this mass loss matches the briquettes that were dried at the 60°. When looking at the briquettes that contained the organic binder, it is shown that they had a higher mass loss and that mass loss increased as their time in the oven increased. These briquettes had a higher mass loss over time than the same briquettes that were dried at the 60° seen in table 4.4

And just like the briquettes dried at the lower temperature, the briquettes dried at the higher temperature were also evaluated for their strength. The strength was tested by drop test, where the briquettes were monitored for when they first broke and when they shattered.

The first group we will look at are the briquettes made with the 2 wt% organic binder.

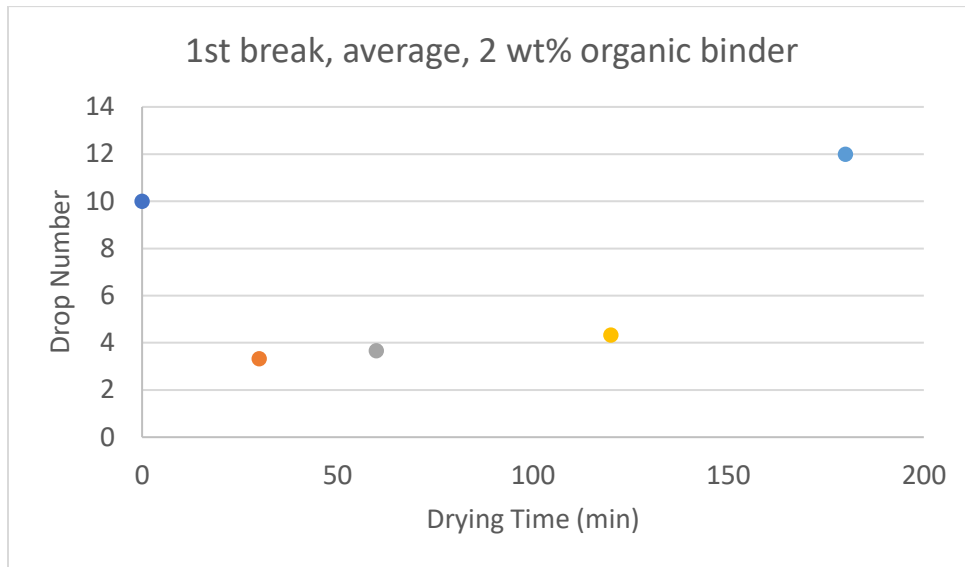


Figure 4.15: First break of briquettes with 2 wt% binder, dried at 80°

When we compare the drying time to a green briquette, the first break number drops significantly for drying up to two hours. When the briquette is kept in for longer (3 hours) the 1<sup>st</sup> break number jumps above the green average. In reviewing the drop number for the briquette to shatter, one sees that the drying time does not really have an effect. One also sees that no matter how long the briquette was in the oven, it took a substantially higher number of drops for the briquette to shatter. It should also be noted that if after the 60<sup>th</sup> drop, if the briquette had not shattered, the test was ended.

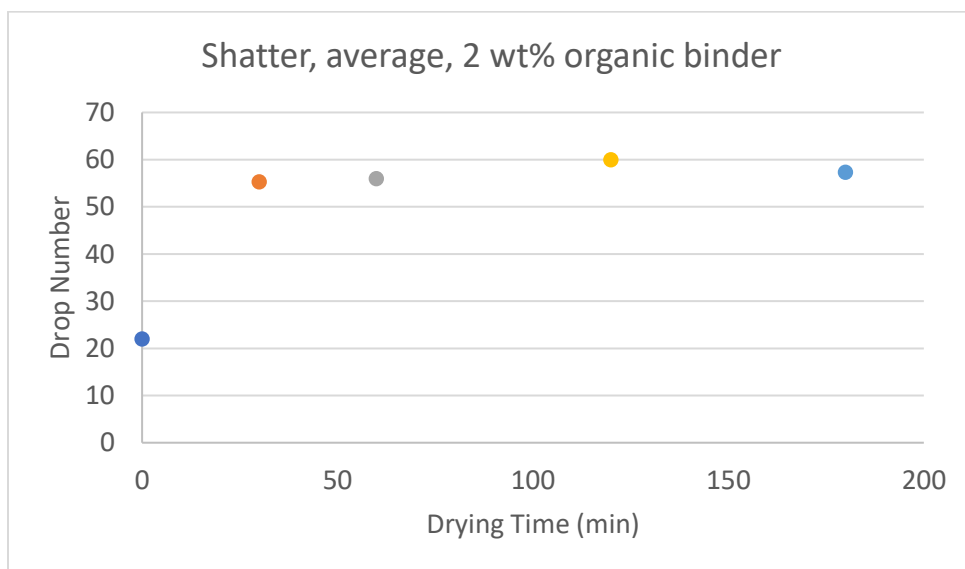


Figure 4.16: Shatter of briquettes with 2 wt% binder, dried at 80°

The next briquettes that were pressed contained 4 wt% organic binder and was dried at 80°, four different times were looked at.

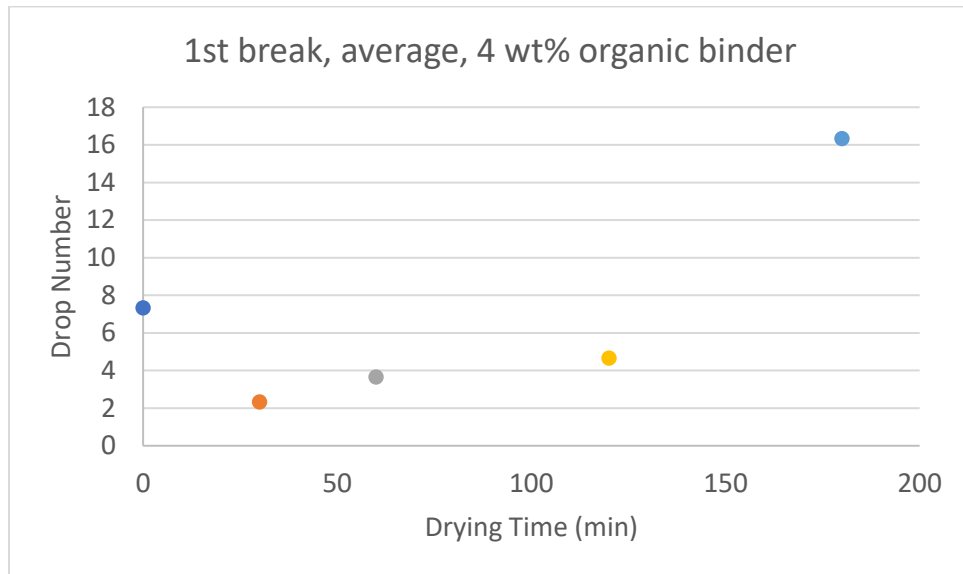


Figure 4.17: First break of briquettes with 4 wt% binder, dried at 80°

When it comes to the first break, the graph, figure 4.17, looks very similar to figure 4.15. Once again, it can be seen that no amount time in the oven outperformed the first three drying times, but does not do better than the briquette that was in the oven for three hours. When looking at the shatter number in figure 4.18 below, one sees that all of the drying times outperformed the green briquette.

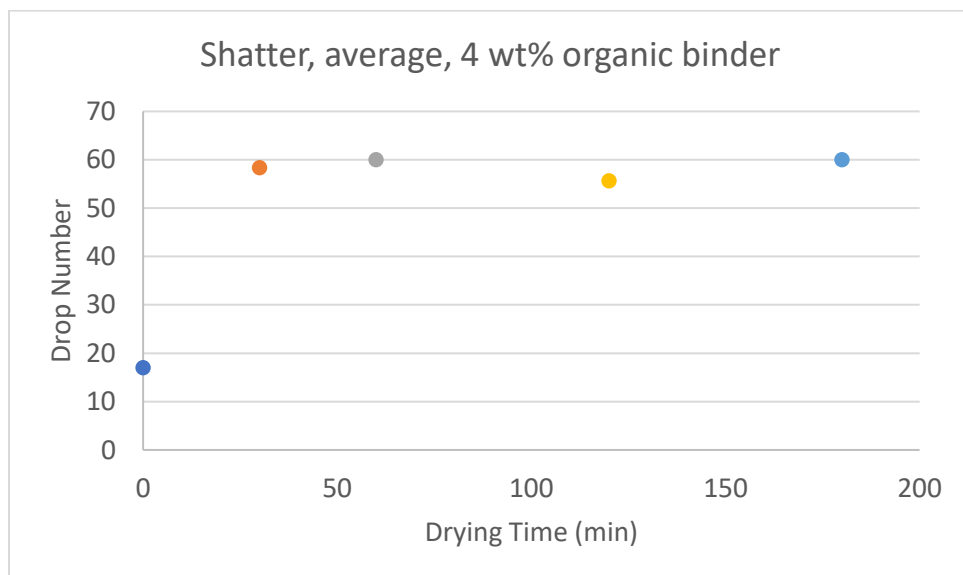


Figure 4.18: Shatter of briquettes with 4 wt% binder, dried at 80°

The last test was for briquettes that were indurated at 80° and contained 6 wt% organic binder.

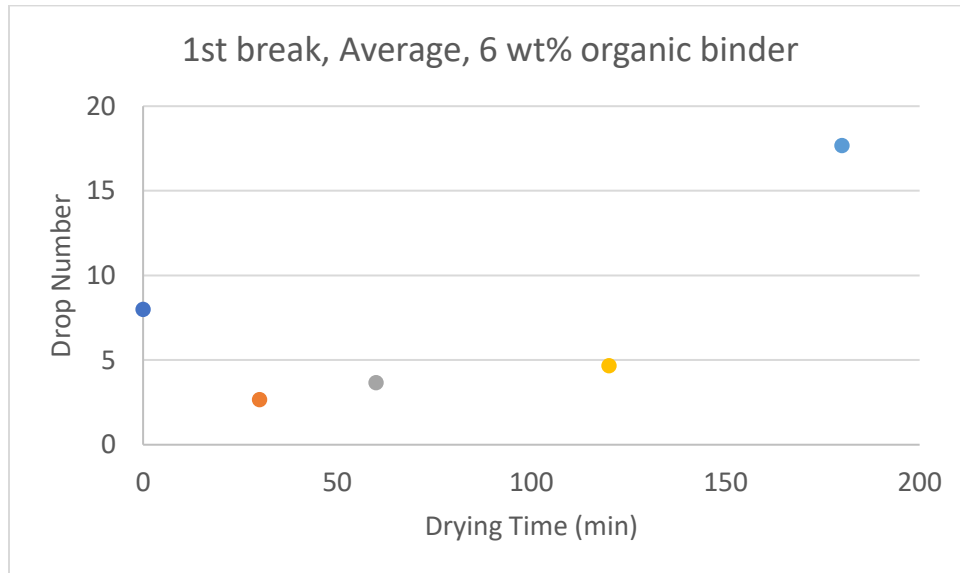


Figure 4.19: First break of briquettes with 6 wt% binder, dried at 80°

In figure 4.19 above, one sees that the longer the briquettes were in the oven the better they performed. While the 1<sup>st</sup> break number increased with drying time, the first three dried samples performed worse than the green briquette. When looking at the shatter number, figure 4.20, one sees that for all four drying times, the performance was essentially the same, with all outperforming the green briquette.

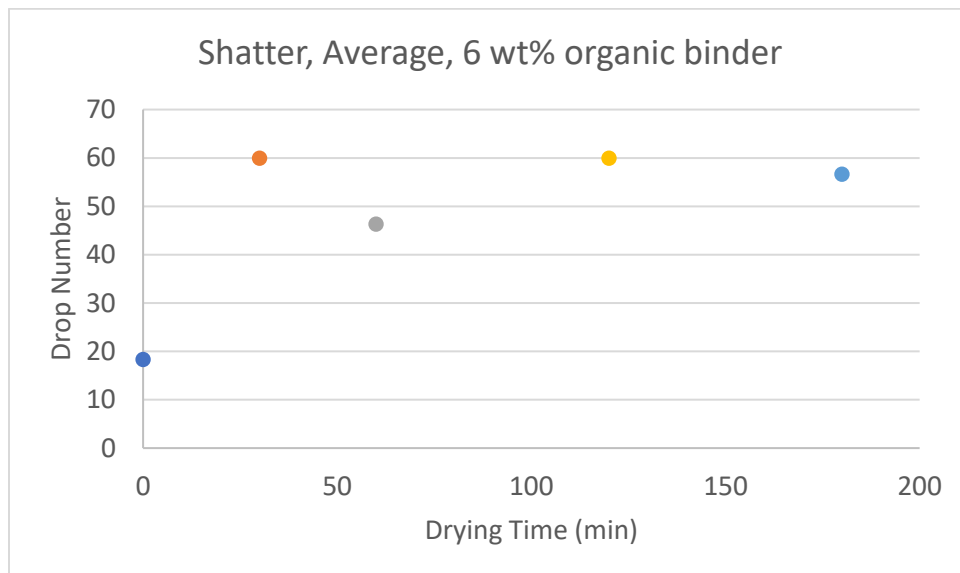


Figure 4.20: Shatter of briquettes with 6 wt% binder, dried at 80°

When comparing the two drying temperatures against each other, using the briquettes that were pressed with 2% organic binder, the data shows that the higher the temperature, the better the performance of the briquettes.

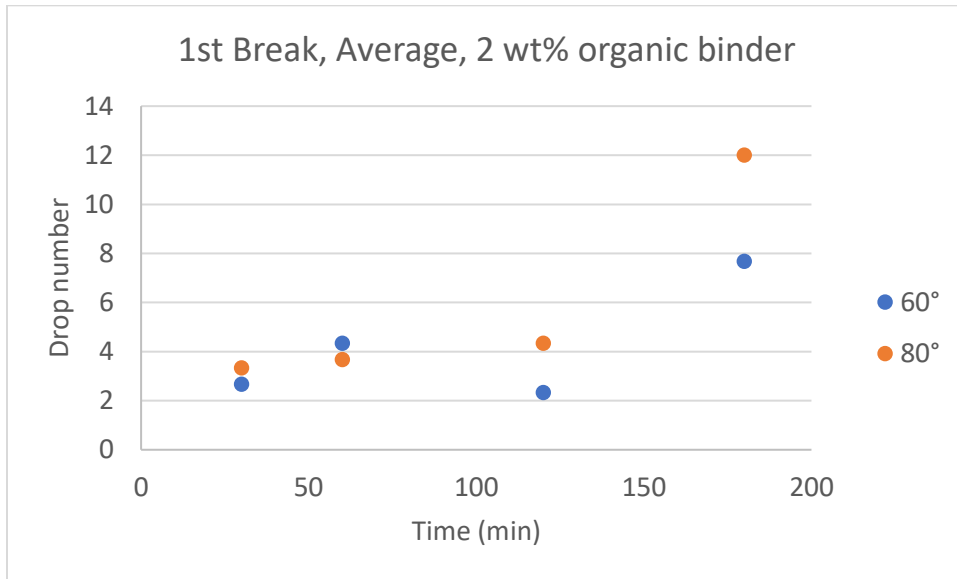


Figure 4.21: Comparison of drying temperature, 2 wt% binder, first break

When looking at the shatter number, the higher temperature briquettes were far superior to the lower temperature ones. One sees that the briquettes indurated at the higher temperature, performed 300% better than the briquettes indurated at the lower temperature.

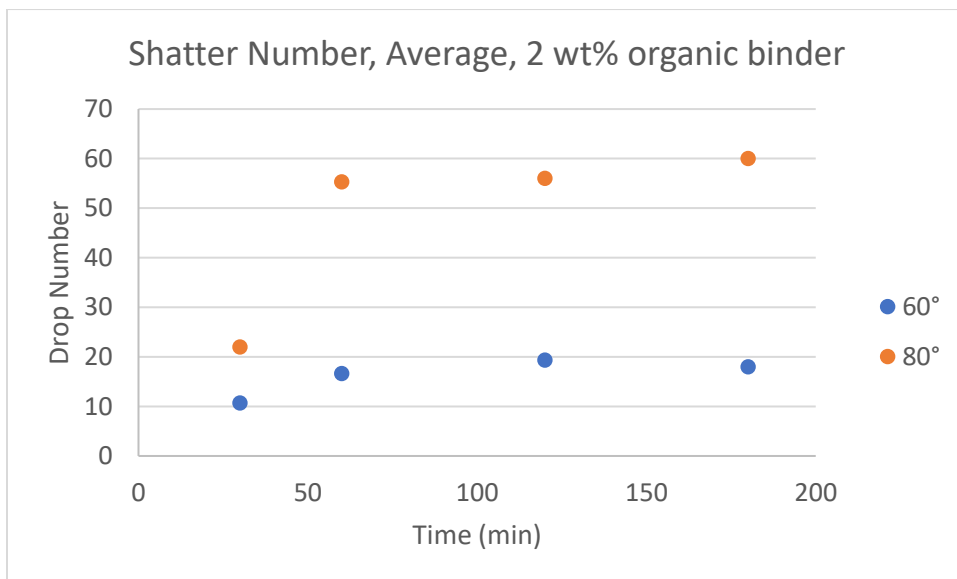


Figure 4.22: Comparison of drying temperature, 2 wt% binder, Shatter

When comparing the visuals of the briquettes dried at 60° to the briquettes at 80° there is one factor that is very noticeable. The briquettes dried at the higher temperature have not only more, but bigger voids than the briquettes dried at the lower temperature.

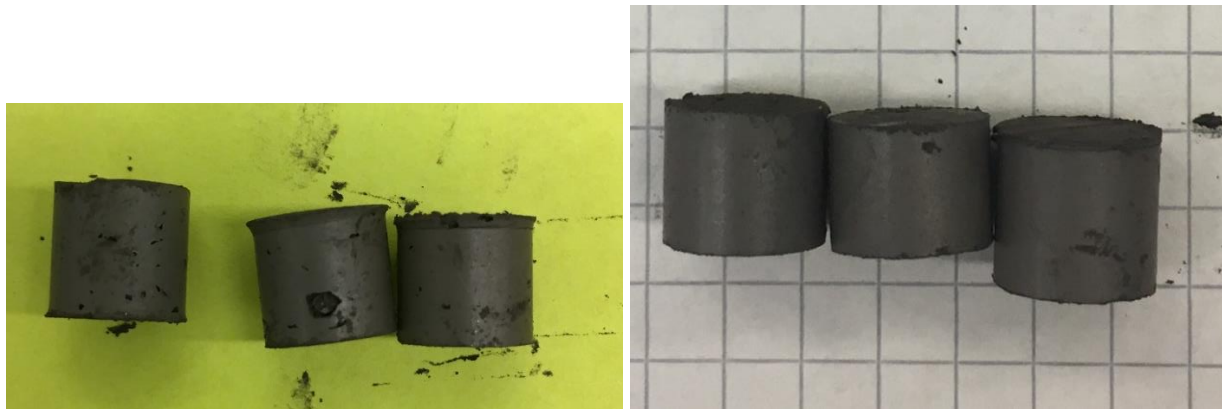


Figure 4.23: Briquettes dried at 80° on the left, Briquettes dried at 60° on the right

#### 4.6 Strength of green pellets

Along with the briquettes, the strength of these green pellets is important to know and understand. The same method that was used for the briquettes was also used for the pellets. A single pellet was dropped from a height of 23cm on to a steel plate. The drop number after the first break was noted and the drop number when the pellet shattered (more than 50% breakage) was noted. The obtained numbers for the two sizes of pellets are presented in Table 4.6.

Table 4.6: Drop test results for green pellets

Size	Water	Organic Binder wt %	1 <sup>st</sup> break	Shatter
1.8	10	6	2	3
1.8	10	6	2	3
1.8	10	6	4	5
4.5	10	6	2	2
4.5	10	6	6	7
4.5	10	6	2	3

It can be seen in the table above that the strength of these green pellets is much lower, especially for the shatter number, than the green briquettes that were tested. One of the reasons for the poor performance could be the shape of the pellets. The pellets that were created were not all uniform in size and shape, some of the pellets came out in more of an oblong shape, as it can be seen in the figure 4.24 below.



Figure 4.24: Example of pellets that were produced

## 4.7 Strength of indurated pellets

The two sizes of pellets produced were dried in the oven for 5 hours at 80°

Table 4.7: Mass loss of pellets dried at 80°

Size	% Binder	% Water	Time	Temp	Mass loss
+1,8mm	6	10	300	80	17.75%
+4.5	6	10	300	80	17.35%

We can see that pellet size did not have much effect on drying as both sizes had essentially the same mass loss. After the pellets were finished drying, they were evaluated for their strength by using the drop test. The pellets were evaluated for when they first broke, the results can be seen in the graph below, figure 4.25.

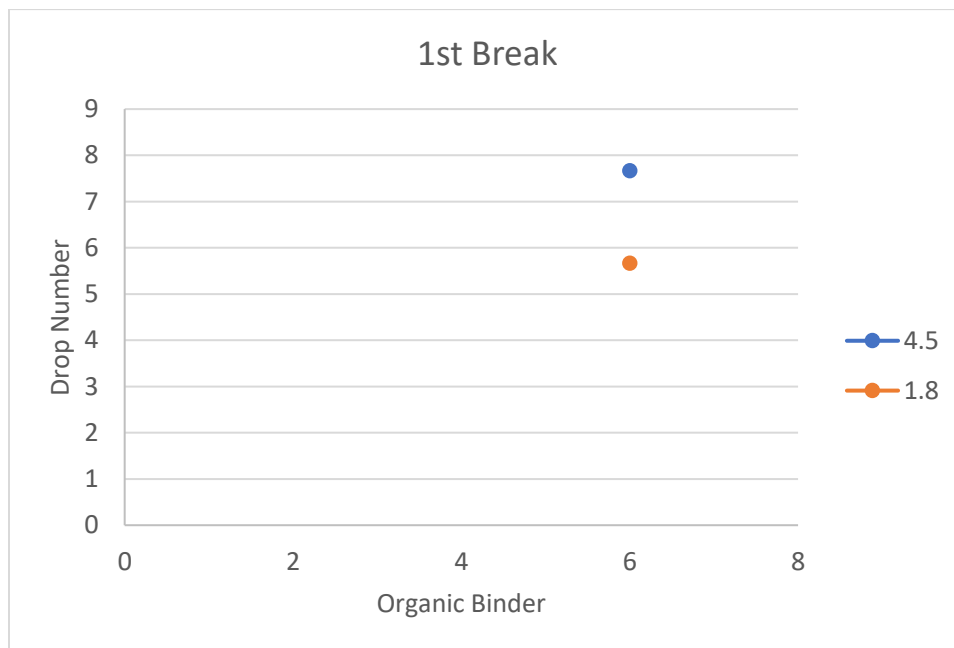


Figure 4.25: First break of dried pellets, 6 wt% binder, 80°

We can see that the larger pellets performed better than the smaller pellets. In comparing these numbers to the numbers in figure 4.19, where the briquettes with 6 wt% organic binder that were dried for 180 min, these pellets performed worse. Here the larger pellets actually performed 70% worse than the briquettes. This trend carries through to the shatter number as well. Looking at the figure below we can see that the smaller pellets performed better than the larger pellets. When comparing to figure 4.20, one sees the larger pellets perform worse than the briquettes. When it comes to the shatter number the larger pellets performed 19% worse than the briquettes.

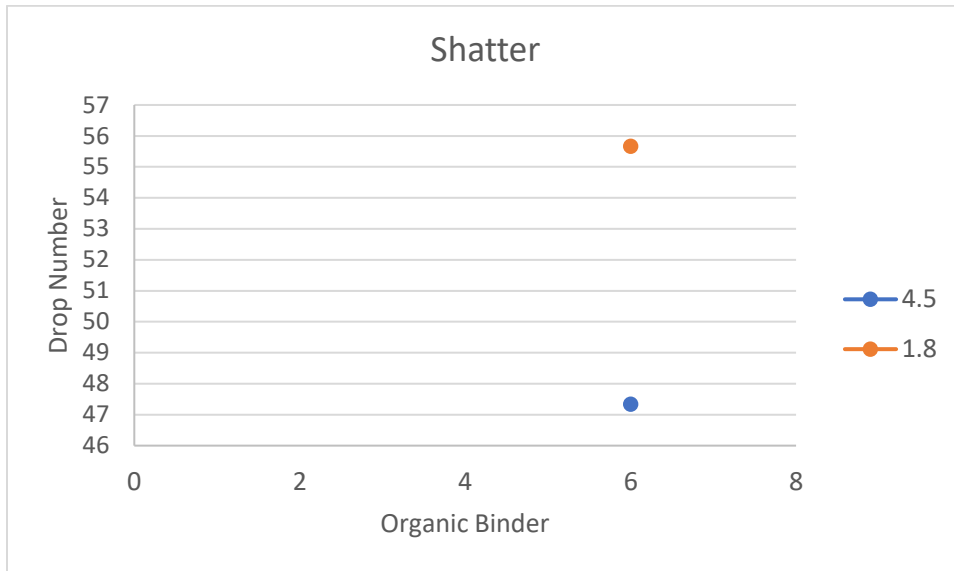


Figure 4.26: Shatter of dried pellets, 6 wt% binder, 80°

## 5 Conclusions and future work

There are many things that can be seen from the research presented above. This section will restate the major findings from above.

### **When looking at the briquettes that were made with only water**

We can see that as you increase the water content, the first break number increases. It should be noted that with that test, there was the error in the pressing and that should be looked at further.

Looking at the shatter number, it can be seen that increasing water content does not equal a higher shatter number. All of the briquettes, no matter their water content, had roughly the same shatter number.

### **When looking at the briquettes that were made with binder**

When looking at the first break number, it can be seen that both the lime and the organic binder when added to the briquettes outperformed the briquettes with only water.

When looking at the shatter number, it can be seen that briquettes with the added binder did not perform better than the briquettes with just the water. It can also be seen that increased binder amounts does not automatically mean an increased shatter number.

### **When looking at the briquettes that were indurated in the oven at 60°**

When looking at both the water and the organic binder, it can be seen that increased drying time will increase the strength of the briquette. This is seen in both the 1st drop number and the shatter number of the briquette.

### **When looking at the briquettes that were indurated in the oven at 80°**

When looking at the first break number, it can be seen that as the drying time increased, so did the performance of the briquette. When the briquette was dried for three hours, it performed better than the green briquette.

When looking at the shatter number drying time did not have that much of an effect. All of the briquettes, no matter their drying time, had excellent performance.

### **Pellets made with a pelletizer.**

The green pellets performed worse than the green briquettes.

The dried pellets had both high first break and shatter number, but the dried pellets performed worse than the dried briquettes.

### **Future Work**

While this project made good advancements, there is still a lot that needs to be looked at. Creating pellets with the pelletizing disk should be investigated. Creating these pellets with different binder amounts and different water content. Creating a more uniform pellet in shape needs to be looked at further. Other tests can be run to evaluate the quality of the briquettes or pellets. Some of these tests are; crushing strength, microporosity, and tumbler resistance. Most of these tests should be done on both the green and indurated agglomerates. As it can be seen in this report, the work was done on a small laboratory scale. The production process of the agglomerates needs to be evaluated at a larger scale and the quality of these agglomerates needs to be checked. After the perfect agglomerate has been determined, the last step that needs to be done would be a plant design and process control measures.

## 6 References

- [1] U.S. Energy Information Administration, “International Energy Outlook,” Sep. 2017.
- [2] “Ambient (outdoor) air quality and health,” *World Health Organization*. [Online]. Available: [http://www.who.int/news-room/fact-sheets/detail/ambient-\(outdoor\)-air-quality-and-health](http://www.who.int/news-room/fact-sheets/detail/ambient-(outdoor)-air-quality-and-health). [Accessed: 15-Jun-2018].
- [3] D. Ciolkosz, “What is Renewable Energy?,” *Penn State Extension*. [Online]. Available: <https://extension.psu.edu/what-is-renewable-energy>. [Accessed: 15-Jun-2018].
- [4] “BP Statistical Review of World Energy 2017.”
- [5] “History of Solar Cells: How Technology Has Evolved,” *Solar Power Authority*, 13-Jul-2016. [Online]. Available: <https://www.solarpowerauthority.com/a-history-of-solar-cells/>. [Accessed: 15-Jun-2018].
- [6] M. Schmela, “Global Market Outlook for Solar Power/2017-2021,” 13-Jun-2017.
- [7] J. Hill, “Global Solar Market Demand Expected To Reach 100 Gigawatts In 2017, Says SolarPower Europe | CleanTechnica,” *Clean Technica*. [Online]. Available: <https://cleantechnica.com/2017/10/27/global-solar-market-demand-expected-reach-100-gw-2017-solarpower-europe/>. [Accessed: 15-Jun-2018].
- [8] M. Munsell, “10 Trends That Will Shape the Global Solar Market in 2018,” 31-Jan-2018. [Online]. Available: <https://www.greentechmedia.com/articles/read/solar-trends-2018-gtm-research>. [Accessed: 15-Jun-2018].
- [9] A. Dong, L. Zhang, and L. N. W. Damoah, “Beneficial and technological analysis for the recycling of solar grade silicon wastes,” *JOM*, vol. 63, no. 1, pp. 23–27, Jan. 2011.
- [10] B. J. Skinner, “Earth resources,” *Proc. Natl. Acad. Sci.*, vol. 76, no. 9, pp. 4212–4217, Sep. 1979.
- [11] A. Schei, J. K. Tuset, and H. Tveit, *Production of High Silicon Alloys*. Tapir, 1997.
- [12] M. Tangstad and L. Kolbeinsen, *Metal production in Norway*. 2013.
- [13] J. Safarian, G. Tranell, and M. Tangstad, “Processes for Upgrading Metallurgical Grade Silicon to Solar Grade Silicon,” *Energy Procedia*, vol. 20, pp. 88–97, Jan. 2012.
- [14] F. ISE, “Photovoltaics Report,” p. 45.
- [15] R. Uecker, “The historical development of the Czochralski method,” *J. Cryst. Growth*, vol. 401, pp. 7–24, Sep. 2014.
- [16] L. Arnberg, M. Di Sabatino, and E. J. Øvrelid, “State-of-the-art growth of silicon for PV applications,” *J. Cryst. Growth*, vol. 360, pp. 56–60, Dec. 2012.
- [17] J. Nelson, *The physics of solar cells*. London : River Edge, NJ: Imperial College Press ; Distributed by World Scientific Pub. Co, 2003.
- [18] T. A. Engh, *Principles of Metal Refining*. Oxford, New York: Oxford University Press, 1992.
- [19] J. Safarian and M. Tangstad, “Vacuum Refining of Molten Silicon,” *Metall. Mater. Trans. B*, vol. 43, no. 6, pp. 1427–1445, Dec. 2012.
- [20] M. A. Green *et al.*, “Solar cell efficiency tables (version 50),” *Prog. Photovolt. Res. Appl.*, vol. 25, no. 7, pp. 668–676.
- [21] M. Di Sabatino, 2017.
- [22] L. Johnsen, J. E. Olsen, T. Bergstrøm, and K. Gastinger, “Heat Transfer During Multiwire Sawing of Silicon Wafers,” *J. Therm. Sci. Eng. Appl.*, vol. 4, no. 3, pp. 031006-031006–7, Jul. 2012.
- [23] C. O. Beale and J. E. Appleby, “Pelletizing,” 1963.

- [24] K. Meyer, *Pelletizing of iron ores*. Berlin; New York: Springer-Verlag, 1980.
- [25] FEECO International, "The agglomeration handbook," 2018.
- [26] T. By, "Briquetting of Manganese Oxide Fines with Organic Binders."